Journal of Medicinal Chemistry

Article

Development of Kinase-Selective, Harmine-Based DYRK1A Inhibitors that Induce Pancreatic Human #-Cell Proliferation

Kunal Kumar, Peng Wang, Roberto Sanchez, Ethan Swartz, Andrew F. Stewart, and Robert J DeVita

J. Med. Chem., **Just Accepted Manuscript** • DOI: 10.1021/acs.jmedchem.8b00658 • Publication Date (Web): 30 Jul 2018

Just Accepted

ACS Publications

is published by the American Chemical Society. 1155 Sixteenth Street N.W., Washington, DC 20036

Development of Kinase-Selective, Harmine-Based DYRK1A Inhibitors that Induce Pancreatic Human β-Cell Proliferation.

*Kunal Kumar[1,2], Peng Wang[3], Roberto Sanchez[1,2], Ethan A Swartz[3], Andrew F. Stewart[3] and Robert J. DeVita[1,2]**

[1] Drug Discovery Institute, Icahn School of Medicine at Mount Sinai, New York, NY 10029, USA

[2] Department of Pharmacological Sciences, Icahn School of Medicine at Mount Sinai, New York, NY 10029, USA

[3] Diabetes, Obesity, and Metabolism Institute, Icahn School of Medicine at Mount Sinai, New York, NY 10029, USA

* Corresponding author: Robert J. DeVita. E-mail: robert.devita@mssm.edu. Phone: 212-659-5542;

KEYWORDS: Dual-specificity Tyrosine-Regulated Kinases (DYRKs), Harmine, DYRK1A inhibitor, Structure Activity Relationship Study, β-cell proliferation, diabetes.

ABSTRACT

DYRK1A has been implicated as an important drug target in various therapeutic areas, inluding neurological disorders and oncology. DYRK1A has more recently been shown to be involved in pathways regulating human β-cell proliferation, thus making it a potential therapeutic target for both Type 1 and Type 2 diabetes. Our group, using a high-throughput phenotypic screen identified harmine that is able to induce beta cell proliferation both *in vitro* and *in vivo*. Since harmine has suboptimal kinase selectivity we sought to expand structure-activity relationships for harmine's DYRK1A activity, to enhance selectivity, while retaining human β-cell proliferation capability. We carried out the optimization of the 1-position of harmine and synthesized 15 harmine analogs. 6 compounds showed excellent DYRK1A inhibition with IC_{50} in the range of 49.5-264 nM. Two compounds, **2-2** and **2-8**, exhibited excellent human β-cell proliferation at doses of 3-30 μM and compound **2-2** showed improved kinase selectivity as compared to harmine.

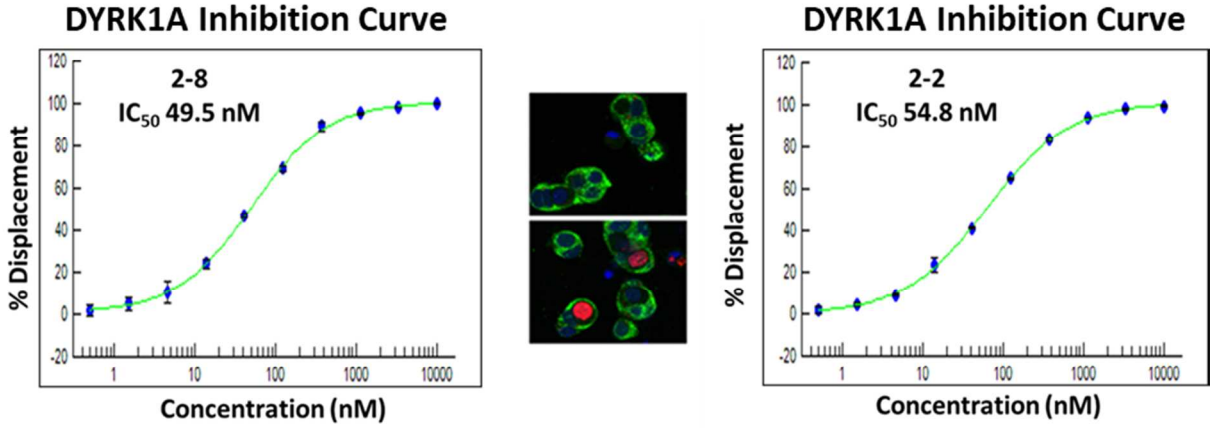

INTRODUCTION:

The Dual-specificity Tyrosine-Regulated Kinases (DYRKs) belong to the CMCG family of eukaryotic protein kinases. The DYRK family consists of five subtypes including 1A, 1B, 2, 3 and 4. Among them, DYRK1A is the most extensively studied subtype. It is ubiquitously expressed and has been shown to play an important roles in brain development and function,[1] neurodegenerative diseases,[2-3] tumorigenesis and apoptosis[4-5] and other cellular functions.. More recently, DYRK1A has been shown to be involved in molecular pathways relevant to proliferation of human insulin-producing pancreatic β-cells, making it a potential molecular target for β-cell regeneration as a therapy to treat Type 1 and Type 2 diabetes.[6-9] DYRK1A inhibition has been proposed to drive pancreatic β-cell proliferation in part by inducing translocation of the nuclear factor of activated T cells (NFAT) family of transcription factors into the nucleus, allowing access to promoters of genes that subsequently activate human β-cell proliferation.[6, 8]

Because of the prominent role of DYRK1A in neurodegenerative disease and cancer, numerous studies have attempted to identify DYRK1A inhibitor scaffolds.[1, 3-7, 9-10] Several DYRK1A inhibitors, like harmine from natural sources, as well as from small molecule drug discovery programs, have been identified and characterized including, epigallocatechin (EGCG) and other flavan-3-ols,[11-12] leucettines,[13-14] quinalizarine,[15] peltogynoids Acanilol A and B,[16] benzocoumarins (dNBC),[17] indolocarbazoles (Staurosporine, rebeccamycin and their analogues),[18] INDY,[19] DANDY,[20] and FINDY,[21] pyrazolidine-diones,[22-23] amino-quinazolines,[24] meriolins,[25-27] pyridine and pyrazines,[28] chromenoidoles,[29] 11H-indolo[3,2-c]quinoline-6-

carboxylic acids,[30] thiazolo[5,4-f]quinazolines (EHT 5372),[31-32] CC-401[33] and 5-iodotubercidin[9, 34]. Among all the DYRK1A inhibitors, harmine and its analogues (β-carbolines) are the most commonly studied and remain the most potent and orally bioavailable class of inhibitors known to date.[3, 10] Historically, harmine is also known to exhibit hallucinogenic properties acting as CNS stimulant, due to its affinity for the serotonin, tryptamine and other receptors.[35-36] Studies have revealed multiple CNS-based effects of harmine, including excitation, tremors, convulsion, and anxiety.[37] Also, harmine and several related analogues have been found to inhibit DYRK1A-mediated phosphorylation of *tau* protein, thought to be relevant to Alzheimers's Disease (AD) and Down's Syndrome (DS, trisomy 21).[38] Harmine has also attracted serious interest for cancer therapy.[39-43] Using systematic structure modifications, several harmine analogues have been identified to show potent anti-proliferative tumor activity, *in vitro* and *in vivo* through multiple mechanisms of action, including inhibition of topoisomerase I,[44-45] inhibition of CDKs,[46] induction of cell apoptosis,[47] and DNA intercalation[48].

Recently, using a luciferase reporter phenotypic high-throughput small-molecule screen (HTS), our group identified harmine as a new class of compounds able to induce human β-cell proliferation, as measured by immunolabeling of insulin producing β-cells, in a range relevant for therapeutic human β-cell expansion.[6] DYRK1A is the most likely target of harmine for β-cell proliferation, as demonstrated by genetic silencing, overexpression and other studies, likely working through the Nuclear Factors of Activated T-cells (NFAT) family of transcription factors that activate cell cycle machinery to cause proliferation while maintaining differentiation in the human β-cell.[6] Using three different mouse, rat and human islet–implant models, it was also shown that harmine is able to induce β-cell proliferation, increase islet mass and improve

glycemic control.[6] Other labs have confirmed these results with other DYRK1A inhibitors unrelated to the harmine scaffold.[7-9]

DYRK1A and NFATs are widely expressed outside β-cells, and harmine analogs are known to have off-target effects, leading to pharmacological side effects thereby limiting the therapeutic utility and potential for pharmaceutical development of harmine analogues for a chronic diseases like diabetes. Thus, there is an urgent need to develop strategies to identify selective harmine analogs specifically designed to induce human β-cell proliferation as pharmacological probes for therapeutic development, with limited off-target activities. In addition, optimized selective harmine analogs may also be useful for specific, targeted delivery to the β-cell. One such prototype technology from DiMarchi and colleagues was recently developed to conjugate estrogen derivatives to GLP-1 analog peptides to effectively target cells that express GLP1-receptor.[49]

With knowledge of this previous work, we explored the binding pockets of known DYRK1A inhibitor-co-crystal structures and identified areas for expansion of the harmine scaffold that will make new contacts to DYRK1A to identify kinase selective as well as linkable harmine analogs for targeted therapy. We carried out the optimization studies of harmine to expand the structure-activity relationships for harmine and to correlate DYRK1A activity, kinase selectivity and human β-cell proliferation. Herein, we report the optimization of harmine 1-position and identification of harmine-based DYRK1A inhibitors that exhibit excellent human β-cell proliferation with improved kinase selectivity as compared to the hit molecule harmine.

RESULTS AND DISCUSSIONS:

Chemistry: The 1-position harmine amine analogs were synthesized by the following reaction

sequence outlined in **Scheme 1**. *m*-Anisidine underwent classical diazotization to form corresponding aryldiazonium salt which was coupled with 3-carboxy-2-piperidone to give arylhydrazone **1-2**.[50] Fisher indole cyclization of the resulting arylhydrazone in the presence of formic acid afforded 1,2,3,4-tetrahydro-1-oxo-β-carboline **1-3**.[50] Oxidation of **1-3** using DDQ followed by chlorination with phosphorous oxychloride generated 1-chloro-β-carboline **1-5** in 79% yield.[51-52] Finally, 1-amino-β-carbolines **1-6** (10 analogs) were prepared via amination of 1-chloro- precursors **1-5** by heating with an excess of neat amine at 170°C in 43-87% yield.[52] Analog **1-6a** was synthesized by Pd catalyzed amination of **1-5** [53] (conversion for this amination was surprisingly low) though provided a sufficient amount of pure compound for *in vitro* assay.

Scheme 1. Synthesis of 1-amino harmine analogs[a]

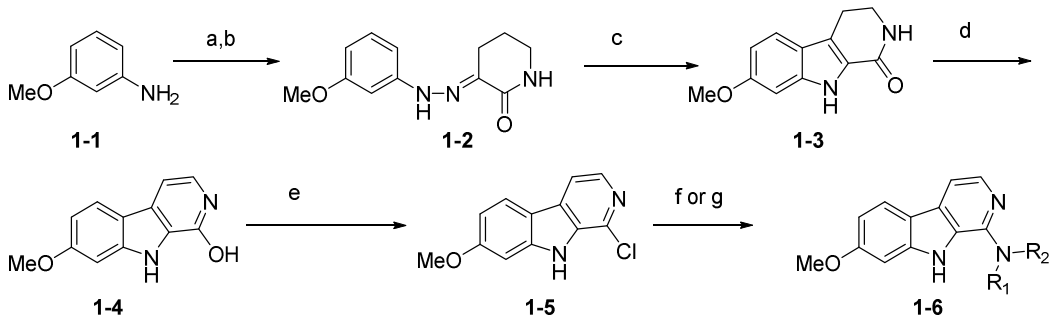

[a]Reagents and conditions: (a) $NaNO_2$ (1.03 eq.), HCl, 10 ^{0}C, 1 h, (b) Ethyl 2-oxopiperidine-3-carboxylate (1.05 eq.), KOH (1.2 eq.), pH adjusted to 4-5, water, rt , 5 h; (c) formic acid, reflux, 1 h; (d) DDQ (1.2 eq.), 1,4-dioxane, 0 °C-rt, 1 h, 23% (4 step); (e) $POCl_3$, 150 °C, 24 h, 79%; (f) R_1R_2NH (10 eq.), 170 °C, 24 h, 43-87% (for **1-6b – 1-6j**); (g) Ruphos (1 mol%), RuPhos Precat (1 mol%), Azetidine (1.2 eq.), LiHMDS (1 M in THF, 2.4 eq.), 90 °C, 96 h, 31% (based on 32 mg (64%) recovered starting material, for **1-6a**).

1-Hydroxymethyl and 3-Hydroxymethyl substituted-β-carbolines were synthesized using the sequences shown in **Scheme 2**. Oxidation of harmine with *m*-CPBA generated the corresponding N-oxide **2-1,** which subsequently underwent Boekelheide rearrangement in the presence of trifluoroacetic anhydride to give the desired 1-hydroxymethyl β-carboline **2-2** as white solid in 49% yield.[54-55] Alternatively, 6-methoxyindole was reacted with oxime **2-3**, prepared from ethyl 3-bromo-2-oxopropanoate, in the presence of sodium carbonate at room temperature to give indole-oxime **2-4**.[56] Oxime reduction of **2-4** with zinc powder in acetic acid then provided tryptophanyl ester **2-5** which was underwent Pictet-Spengler cyclization with acetaldehyde to provide 1-methyl-3-hydroxymethyl tetrahydro-β-carboline **2-6**.[56-57] Aromatization of compound **2-6** followed by reduction of the ester afforded the final compound **2-8** as white solid.[57] Reduction of **2-8** using Et_3SiH and $PdCl_2$ as catalyst afforded 1,3-dimethyl-7-methoxy-β-carboline **2-9** as white solid.[58]

Scheme 2. Synthesis of 1-hydroxymethyl and 3-hydroxymethyl harmine analogs[a]

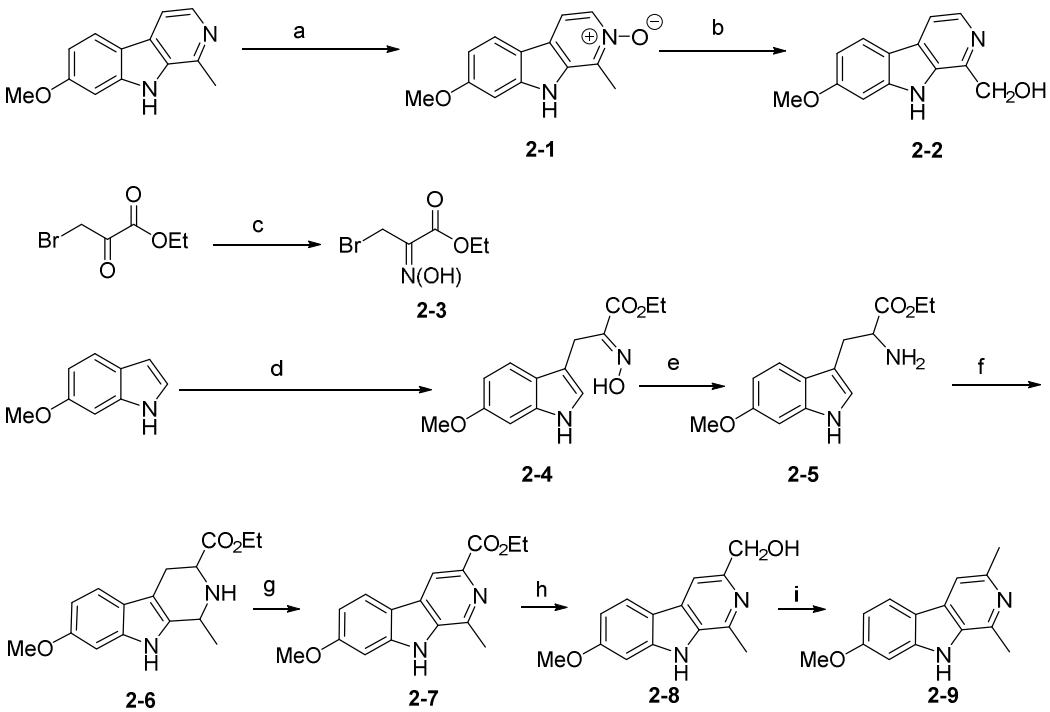

[a]Reagents and conditions: (a) *m*-CPBA (3 eq.), MeOH, $CHCl_3$, 70 ^oC, 12 h, 47%; (b) TFA anhydride (2.5 eq.), CH_2Cl_2, reflux, o/n, 49%; (c) $N_2H_4OH.HCl$ (1 eq.), MeOH, $CHCl_3$, rt, 24h, 81%; (d) **2-3** (1 eq.), K_2CO_3 (5.5 eq.), DCM, rt, 48 h, 34%; (e) Zn dust, AcOH, rt, o/n, 96%; (f) Acetaldehyde (1 eq.), TFA (5%), DCM, rt, o/n; (g) S_8 (2 eq.), Xylene, reflux,o/n, 75%; (h) $LiAlH_4$ (2 eq.), THF, rt, 12 h, 91%; (i) Et_3SiH (16 eq.), $PdCl_2$ (0.2 eq.), EtOH, 90 ^oC, 5 h, 27%.

Synthesis of 1-(1-hydroxy)ethyl and 1-acetyl harmine analogs are outlined in **Scheme 3**. 6-methoxy tryptamine underwent Pictet-spengler cyclization with pyruvic aldehyde in presence of 5 % TFA to provide 1-acetyl-7-methoxy-tetrahydro-β-carboline **3-1**. Aromatization of compound **3-1** followed by reduction of the acetyl group afforded the 1-(1-hydroxyethyl) harmine analog **3-3** as white solid in 49% yield.

Scheme 3. Synthesis of 1-(1-hydroxy)ethyl and 1-acetyl harmine analogs[a]

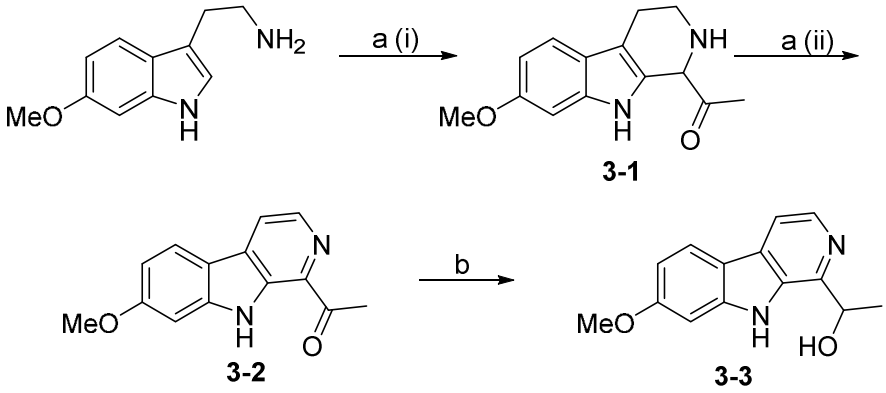

[a]Reagents and conditions: (a) (i) pyruvic aldehyde (1.2 eq.), TFA (5%), DCM, rt, 12 h; (ii) $KMnO_4$ (4 eq.), THF, rt, 12 h, 16% (2 steps); (b) $NaBH_4$ (2 eq.), MeOH, rt, 12 h, 49%.

Structure-Activity Relationship Studies of Harmine Analogs: Harmine is a type I DYRK1A inhibitor that binds to the ATP binding pocket and forms hydrogen bonding interaction with both the side chain of Lys188 and backbone of Leu241 (**Figure 1A**).[19] Recently, the crystal structure of an ATP-competitive inhibitor DJM2005 bound to DYRK1A was also reported.[59] These data

showed classical binding to the ATP site with the inhibitor forming hydrogen bond interactions with the backbone of Leu241 along with water-mediated contacts with the side chains Lys188, Glu203 and the backbone of Asp307 (**Figure 1B**). Interestingly, the primary amino group of DJM2005 was also shown to form two additional hydrogen bonds with the side chains of Asn292 and DFG motif Asp307.[59] Moreover, it was also observed that movement of Phe170 in the DYRK1A-DJM2005 complex, creating another "induced-fit"pocket which is occupied by the chlorophenyl group (**Figure 1C, 1D**). In comparison, harmine binds in ATP-binding site without accessing this additional space occupied by DJM2005. Hence, we proposed rational modifications of the 1-position of harmine to access this pocket to identify new harmine based DYRK1A inhibitors with the potential to be chemically linked to GLP-1 agonists, for example, for β-cell targeted delivery. Modifications of the 1-position in harmine have been explored previously[52, 60-61], but not in the context of diabetes and β-cell proliferation. A total of 15 harmine analogs were synthesized following the routes described in **Schemes 1 2,** and **3**. DYRK1A binding activity of these analogs was screened using FRET-based LanthaScreen binding assay (Life Technologies), initially at two concentrations:1000 nM and 300 nM. Those compounds showing ≥ 50% inhibition at 300 nM were titrated using ten serial three-fold dilutions (in duplicate) for IC_{50} determination.

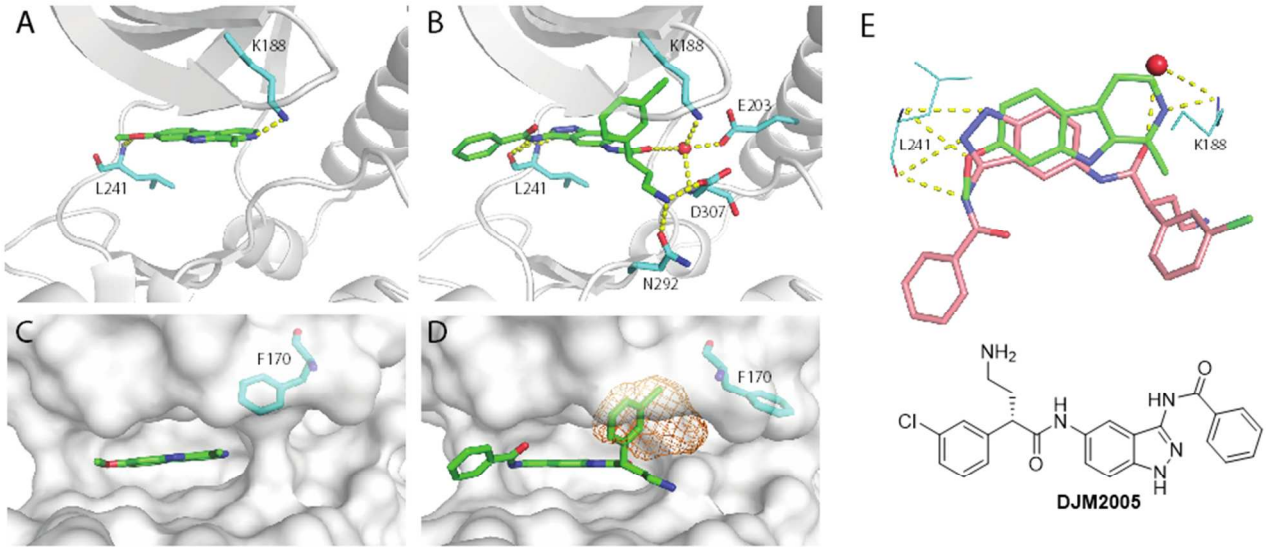

Figure 1. Comparison of Harmine and DJM2005 binding to DYRK1A. **(A)** Harmine binds in the ATP-binding pocket of DYRK1A making hydrogen bonding contacts (yellow dashed lines) with the side chain of Lys188 and the backbone of Leu241 (PDB 3ANR). **(B)** DJM2005 also interacts with the backbone of Leu241 and makes water-mediated contacts with the side chains Lys188, Glu203 and the backbone of Asp307. Additionally, the primary amino group interacts with the side chain of Asn292 and Asp307 (PDB 2WO6). **(C) (D)** The movement of Phe 170 in the DJM2005 complex (**D**) creates a pocket (orange mesh) that is occupied by the chlorophenyl group of DJM2005. **(E)** Superposition of the harmine (green) and DJM2005 (pink) complexes, highlighting the equivalent hydrogen bonding interactions with Leu241 and Lys188. Orientation is rotated 90 degrees with respect to the view in panels **C** and **D**.

Based on our computational modeling, we investigated the effects of cycloalkylamines at the 1-position of harmine on DYRK1A binding. First, we studied three analogs with azetidine (**1-6a**), pyrrolidine (**1-6b**) and piperidine (**1-6c**) substituents at the 1-position. Compound **1-6a** showed the best activity with IC_{50} of 159 nM. However, this compound was 5-fold less active than harmine. Increasing the ring size to 5-membered (pyrrolidine, **1-6b**) and 6-membered

(piperidine, **1-6c**) ring reduced the DYRK1A inhibitory activity, with DYRK1A IC_{50} of 264 nM and 1500 nM, respectively. We also synthesized 7 analogues from commercially available building blocks bearing substituents on the pyrrolidine at harmine 1-position to interrogate the induced binding pocket implicated by the structure of DJM2005 complex. As predicted, the substitution pattern on the pyrrolidine ring was very sensitive to the DYRK1A inhibition activity. Among these analogues, **1-6d** and **1-6f** showed modest DYRK1A inhibition activity. 2-Substituted pyrrolidine analogs were more potent inhibitors as compared to their 3-substituted analogs. Compound **1-6d** with 2-phenyl pyrrolidine substituent showed a DYRK1A IC_{50} of 123 nM comparable to **1-6a** (azetidine), and a 2-fold improvement over the corresponding analog **1-6b**. Unfortunately, introduction of a 3-chloro group, analogous to DJM2005, on 2-phenyl of the pyrrolidine 1-harmine analog was detrimental for the activity (compound **1-6i**, 22% inhibition at 300 nM.), thus demonstrating that harmine-based analogs with directly attached 1-position cycloalkyamines are unable to productively access the induced fit pocket of DJM2005.

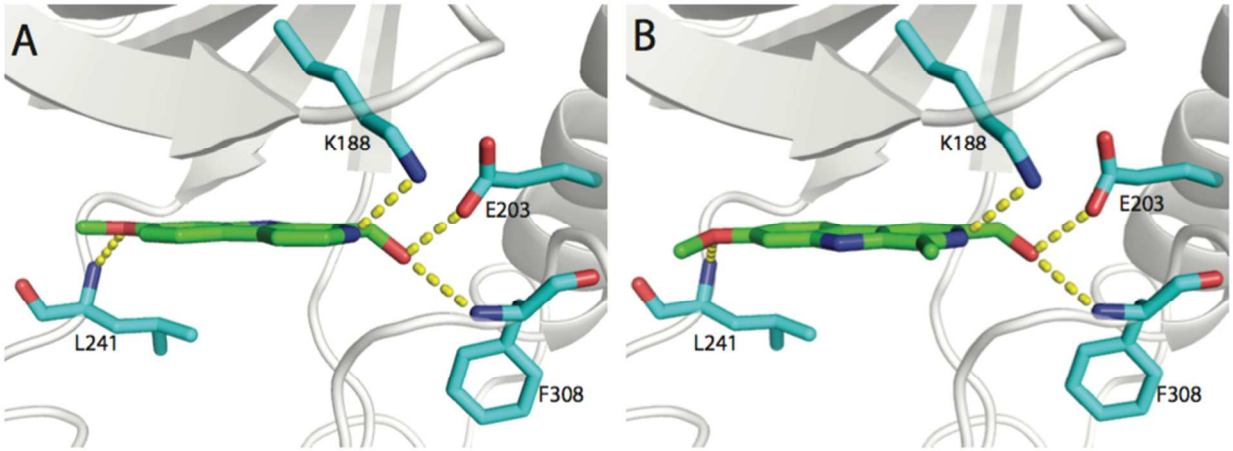

Figure 2. Binding Model of 1-hydroxymethyl harmine Analogs to DYRK1A. (A) Induced fit docking of compound **2-2** predicts that it adopts a binding mode that is distinct from harmine (see **Figure 1A**). The model shows that the hydroxymethyl group at the 1-position causes the scaffold to flip 180° *horizontally*, enabling new putative contacts with the side chains of Glu203

and Phe308, inaccessible to harmine. The model also shows retention of the original hydrogen bonds of harmine 2-nitrogen with Lys188 and 7-methoxy oxygen with Leu241, respectively. Hydrogen bonds are shown as yellow dashed lines (PDB 3ANR). **(B)** Induced fit docking of compound **2-8** predicts that repositioning of the hydroxymethyl group to position-3 causes this compound to revert to the canonical harmine ATP-site binding mode, while creating new contacts from the 3-hydroxymethyl group with Glu203 and Phe308 proposed for the "flipped" binding mode for **2-2** (PDB 3ANR).

Simple replacement of the harmine 1-methyl group with a chlorine atom (**1-5**) significantly improved the DYRK1A inhibition by 3-fold compared to harmine with IC_{50} of 8.81 nM (reported in literature IC_{50} 56 nM)[60]. We also investigated the effect of introducing polar groups like hydroxyl, hydroxymethyl and acetyl at the 1-position of harmine. Replacing 1-methyl with a hydroxyl substituent (or its pyridone tautomer) dramatically reduced the DYRK1A inhibition, rendering the compound inactive, unlike the Cl-subsitutent.

Interestingly, in contrast to a directly attatched hydroxyl group, introduction of 1-hydroxymethyl group (**2-2**) showed potent DYRK1A inhibition with IC_{50} of 55 nM (reported in lietrature IC_{50} 106 nM)[60], comparable but slightly less potent than harmine and a 2-fold improvement over 1-(2-phenylpyrrolidin-1-yl) harmine analog **1-6d**. We studied the binding pose of this compound to DYRK1A by induced fit docking and observed that it adopts a new binding pose that is distinct from the classical ATP-binding pose for harmine (**Figure 1A**). Based on the induced fit modeling, the 1-hydroxymethyl substituent causes the core scaffold to horizontally flip by 180^{o}, creating the possibility for the hydroxyl group to form two new hydrogen bonding interactions with the side chain of Glu203 and the backbone of Phe308 while maintaining the canonical hydrogen bonding interactions with Leu241 and Lys188 (**Figure 2A**).

In order to retain this new hydrogen bond interaction while maintaining the canonical binding pose of harmine, a "non-flipped" version of compound **2-2** with a hydroxymethyl group at the 3-carboline position of harmine (compound **2-8**) was synthesized as shown in the (**Figure 2B**). Induced fit docking of compound **2-8** predicted that repositioning of the hydroxymethyl group to the 3-position would cause it to revert to the canonical harmine binding mode. We were gratified to learn that 3-hydroxymethyl substituted analog **2-8** showed IC_{50} of 49.5nM, comparable to compound **2-2**. Removal of the hydroxyl group (3-methyl carboline analog **2-9**) caused a significant decrease in the DYRK1Abinding affinity with an IC_{50} = 971 nM. These data indicate the importance of the hydroxyl group in **2-8**, further corroborating our modeling results.

Table 1. DYRK1A inhibition and β-Cell proliferation of harmine analogs

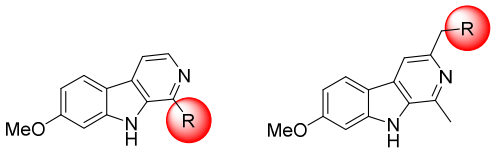

1-4,1-5, 1-6a to 1-6j, 2-2 2-8, 2-9

Compound	R	% DYRK1A inhibition		IC_{50} (nM)[a]	Compound	R	% DYRK1A Inhibition		IC_{50} (nM)[a]
		1000 nM	300 nM				1000 nM	300 nM	
	Harmine	nd	nd	28					
1-6a		89	72	159	1-6i	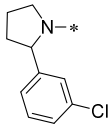	22	1	nd
1-6b		97	90	264					
1-6c		81	57	1500	1-6j	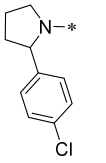	60	27	nd
1-6d		91	71	123					
					1-5	Cl—*	100	98	8.8
1-6e	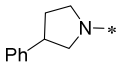	61	34	nd	1-4	HO—*	38	17	nd
1-6f		84	57	221	2-2		75	49	54.8
					2-8	HO—*	98	90	49.5
1-6g	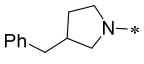	38	15	nd	2-9	—*	-	-	971
1-6h	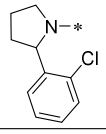	49	12	nd	3-2		92	85	66.7
					3-3		67	38	858

a = IC_{50} values are determined using ten serial three fold dilutions (in duplicate)
nd = not determined

Introduction of an alpha methyl group to the 1-hydroxymethyl substituent of harmine **3-3** led to a complete loss of DYRK1A binding activity at the screening concentration while the planar 1-acetyl substituted analog (**3-2**) had an IC_{50} (66.7 nM) similar to compounds **2-2** and **2-8**. This indicates that the 1-hydroxymethyl group of **2-2** occupies constrained space that does not accommodate further steric bulk, a possibility to have binding mode similar to either **2-2** or **2-8**.

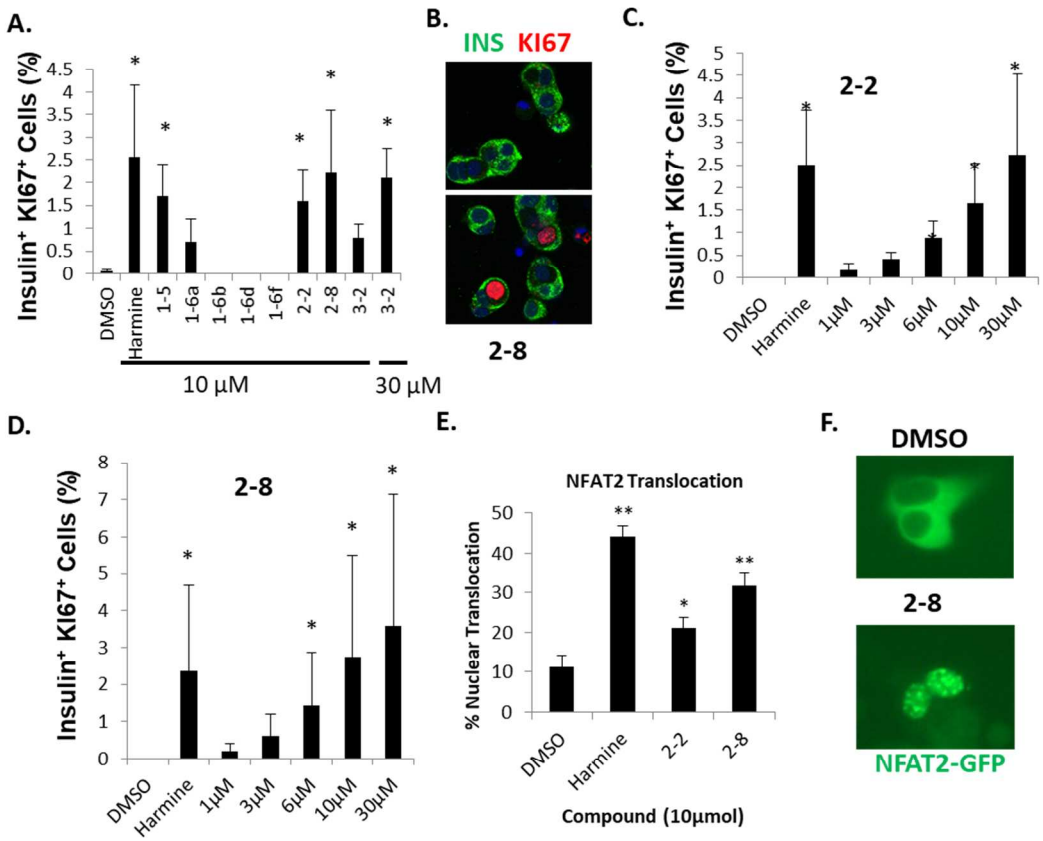

Figure 3. Effects of harmine analogs on human beta cell proliferation. (A) Initial screening of harmine analogs on human beta cell proliferation at 10 µM. DMSO was used as negative control and harmine was used as positive control (n = 4-5). **(B)** A representative example from A of a Ki-67 and insulin double positive cells induced by analog **2-8**. **(C)** and **(D)** Dose-response curves for **2-2** and **2-8** in

human β cells (n = 4 for each dose, harmine concentration 10 μM). **(E)** Quantification of nuclear frequency of NFATC1-GFP in R7T1 rodent beta cell lines treated with harmine, **2-2** and **2-8** (10 μM, 24 hr; n = 3 for each compound). **(F)** A representative example of **2-8** (10 μM, 24 hr) increasing the nuclear frequency of NFATC1-GFP in R7T1 rodent beta cells. In all relevant panels, error bars indicate SEM and, * indicates $P < 0.05$. A minimum of 1,000 beta cells was counted for each graph.

Human β-cell proliferation assay: Eight compounds, **1-5**, **1-6a**, **1-6b**, **1-6d**, **1-6f**, **2-2**, **2-8** and **3-2** which showed DYRK1A inhibition IC_{50} < 250 nM were assessed for their ability to induce human β-cell proliferation *in vitro*. Among these harmine analogs, compounds **2-2**, **2-8** and **1-5** exhibited human β-cell proliferation at 10 μM comparable to that of harmine, as measured by Ki67 immunolabeling (**Figure 3A**). A representative example of a Ki-67 and insulin double positive cells induced by analog **2-8** is shown in **Figure 3B** as per our literature protocols.[6] Compound **3-2** with acetyl substituent at the harmine 1-position, despite having an IC_{50} comparable to **2-2** and **2-8**, showed reduced β-cell proliferation at 10 μM. However, when the compound was tested at higher concentration of 30 μM, proliferation in the range comparable to harmine was observed. Both the compounds **2-2** and **2-8** caused proliferation in a dose-dependent manner (**Figure 3C, 3D**) with compound **2-8** showing superior human β-cell proliferation at lower dose as compared to **2-2**. Unlike harmine, which causes beta cell toxicity at doses higher than 10 μM, compound **2-2** and **2-8** did not cause toxicity even at 30 μM. Compounds **2-2** and **2-8** also drove NFAT2 translocation in rat cell line that transiently transduced NFAT-GFP fusion genes to nucleus as observed for harmine. Collectively, these observations indicate that these compounds drive β-cell proliferation qualitatively like harmine, by inducing translocation of NFATs to the nucleus, likely allowing access to promoters of genes that subsequently drive human β-cell proliferation (**Figure 3E, 3F**).

Interestingly, except for **1-6a**, the 1-amino substituted harmine analogs **1-6b**, **1-6d** and **1-6f** did not show any β-cell proliferation despite showing DYRK1A inhibition < 270 nM, which may indicate a DYRK1A potency threshold for β-cell proliferation. An alternate rationale may be that some of the compounds with reduced β-cell proliferation, such as **1-5** and **1-6a**, may have activity on anti-proliferative kinases in addition to DYRK1A that limit their β-cell proliferative capability. Furthermore, we also may suggest that the difference between *in vitro* DYRK1A binding and the human beta cell proliferation assay might be attributed to physicochemical properties such as, cell permeability and other physical chemical properties of the 1-6 harmine analogues. Studies to address these rationales are on-going.

Table 2. Kinome scan of compound 2-2, 2-8 and harmine[a]

Target	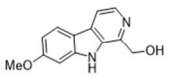 2-2	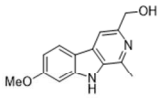 2-8	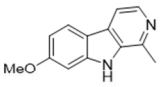 Harmine
CDK11	98	4.8	83
CDK7	27	0.65	21
CDK8	94	0	55
CDKL5	100	6.1	100
CIT	44	8.1	29
CLK1	3.5	7.2	0.35
CLK2	5.5	1.8	2.4
CLK4	17	5	13
CSNK1A1	10	7.8	15
CSNK1D	17	8	13
CSNK1E	6.5	1	1.7
CSNK1G2	30	18	19
CSNK2A1	34	8.3	11
CSNK2A2	37	2.3	23
DAPK1	85	8.8	78
DAPK2	80	2.8	72
DAPK3	81	1.4	69
DRAK2	88	11	73
DYRK1A	0	0	0
DYRK1B	66	0.35	6.1
DYRK2	6.5	4.1	3.2
HASPIN	4.8	0.75	2
HIPK1	30	2.7	21
HIPK2	30	1.3	8.6
HIPK3	21	2.1	9.4
IRAK1	32	18	17
IRAK3	39	70	15
PIK4CB	3.7	19	12
PIM1	65	19	45
PIM2	58	4.7	39
PIP5K2C	28	5	36
RPS6KA4(Kin.Dom.2-C-terminal)	54	1	40
TGFBR2	91	17	78
VPS34	53	28	13

≤ 10
11≤ 20

a = compounds were screened 10 µM against 468 kinases using Discoverx Kinome Scan. Results for primary screen binding interactions are reported as '% DMSO Control', where lower values indicate stronger affinity (see the Supporting Information for details).

Kinome scan profile: As previously mentioned above, harmine is known to exhibit varying degrees of inhibition for kinases other than DYRK1A. In order to understand kinase selectivity, we carried out a kinome profiling of compound **2-2**, **2-8** and harmine on 468 kinases at 10 µM concentration (**Table 2**, more potent activities < 20% remaining colored as shown). Harmine inhibited 17 kinases (<20% activity remaining) in addition to DYRK1A at a screening

concentration of 10 μM similar to earlier reports. Compound **2-2** exhibited a cleaner kinome profile as compared to harmine with significantly reduced inhibition against DYRK1B, CSNK1G2, CSNK2A1, HIPK2, HIPK3, IRAK1, IRAK3 and VPS3 at 10 μM. Additionally, in comparison to harmine, it showed affinity greater than harmine to only PIK4CB at the screening concentration (3.7 vs 19 % activity remaining for **2-2** and harmine, respectively; see Supplementary Information for complete Discoverx screening data). Interestingly, the kinome profile observed for compound **2-8** was much less elective than that of both harmine and **2-2.** In addition to the kinases for which harmine and **2-2** showed inhibition, compound **2-8** exhibited inhibition of several additional kinases including CDKs, DAPKs and PIMs (<20% activity remaining). Despite having poor kinome selectivity profile, it is interesting to note that compound **2-8** showed β-cell proliferation activity and DYRK1A inhibition comparable to harmine and **2-2**. One probable explaination could be that some of these kinases have compensatory mechanism to either induce or inhibit β-cell proliferation. The kinome profile data indicates that between the two harmine scaffold analogs **2-2** and **2-8**, which have similar β-cell proliferation activity and DYRK1A binding, compound **2-2** has improved kinase selectivity thus making it the lead compound for further studies.

CONCLUSIONS:

We have reported the structure-activity relationships of DYRK1A inhibition and β-cell proliferation for new harmine analogs using an integrated, structure-based drug design, computational modeling and medicinal chemistry optimization approach. In order to access the putative induced binding pocket occupied by DJM2005, we synthesized several 1-amino harmine analogs (**1-6a** to **1-6j**) to investigate their effect on DYRK1A kinase binding and human β-cell proliferation. Most of the 2-amino harmine compounds showed reduced DYRK1A inhibition

activity at the screening concentration of 1 μM with the exceptions of harmine analogs **1-6a**, **1-6b**, **1-6d**. These analogs showed a range of 5- to 9-fold reduced DYRK1A inhibitory activity as compared to harmine, indicating that harmine-based analogs with cycloalkylamines directly attached at the 1-position are unable to productively access the induced fit pocket of DJM2005, suggesting alternate linking groups need to be explored.

In contrast, we have shown that harmine analogs **2-2, 2-8** and **3-2** bearing small polar groups like, hydroxymethyl or acetyl exhibited potent DYRK1A inhibition with IC_{50} in the range of 49-67 nM, 2-fold more active than 1-azetidine harmine analog **1-6b**. However, introduction of the directly attached 1-hydroxy substituent (or its pyridone tautomer) was detrimental for DYRK1A inhibition. Interestingly among all the harmine analogs synthesized, the 1-chloro substituted harmine analog (**1-5**) significantly improved DYRK1A inhibition and was the most potent DYRK1A inhibitor compound, with an IC_{50} of 8.8 nM, though it was not explored further as a lead due to its potential for nucleophilic substitution. Among the 8 compounds with IC_{50} < 250 nM against DYRK1A, (**1-5**, **1-6a**, **1-6b**, **1-6d, 1-6f**, **2-2**, **2-8 3-2**) only **1-5, 2-2, 2-8** and **3-2** exhibited human β-cell proliferation comparable to that of harmine at similar or reduced concentrations. Importantly, harmine analogs **2-2** and **2-8** were most effective for inducing human β-cell proliferation *in vitro*, indicating that introduction of polar groups like hydroxymethyl at 1- and 3-positions of harmine improves the β-cell proliferation, possibly by improving kinase selectivity, as shown for **2-2**. None of the 1-amino harmine analogs caused any β-cell proliferation. Kinome scan of 468 kinases for compound **2-2** and **2-8** indicated that compound **2-2** exhibits a cleaner kinome profile as compared to harmine and **2-8** at a concentration of 10μM. In contrast, compound **2-8** exhibited much lower kinase selectivity, inhibiting several additional kinases including CDKs, DAPKs and PIMs (<20% activity remaining).

These data indicate the potential for improvement of the harmine scaffold for kinase selectivity, resulting in β-cell proliferation at lower concentration *in vitro*, with the potential for a cleaner off-target profile. We have been able to successfully modify harmine to identify a novel kinase selective DYRK1A inhibitor **2-2** with improved kinase selectivity and β-cell proliferation ability. These observations suggest that further improvements in DYRK1A binding affinity as well pharmacological studies in addition to DYRK1A binding of the harmine analog series is an attractive approach to the development of effective and novel diabetes therapeutics for β-cell proliferation. The results of our on-going structure-based drug design, medicinal chemistry SAR and pharmacological studies will be reported in due course.

EXPERIMENTAL:

Materials and Methods. ^{1}H and ^{13}C NMR spectra were acquired on a Bruker DRX-600 spectrometer at 600 MHz for ^{1}H and 150 MHz for ^{13}C. TLC was performed on silica coated aluminum sheets (thickness 200 μm) or alumina coated (thickness 200 μm) aluminum sheets supplied by Sorbent Technologies and column chromatography was carried out on Teledyne ISCO combiflash equipped with a variable wavelength detector and a fraction collector using a RediSep Rf high performance silica flash columns by Teledyne ISCO. LCMS/HPLC analysis for purity determination and HRMS was conducted on an Agilent Technologies G1969A high-resolution API-TOF mass spectrometer attached to an Agilent Technologies 1200 HPLC system. Samples were ionized by electrospray ionization (ESI) in positive mode. Chromatography was performed on a 2.1 × 150 mm Zorbax 300SB-C18 5-μm column with water containing 0.1% formic acid as solvent A and acetonitrile containing 0.1% formic acid as solvent B at a flow rate of 0.4 mL/min. The gradient program was as follows: 1% B (0−1 min), 1−99% B (1− 4 min),

and 99% B (4−8 min). The temperature of the column was held at 50 °C for the entire analysis. The purity of all the compounds were ≥ 95%. The chemicals and reagents were purchased from Aldrich Co., Alfa Aesar, Enamine, TCI USA. All solvents were purchased in anhydrous from Acros Organics and used without further purification.

Molecular Modeling: All molecular modeling procedures were carried with the small-molecule drug discover suite of Schrödinger LLC, release 2016-3. The Induced Fit Docking[62] (IFD) protocol combining Glide and Prime was used to dock the compounds using the crystal structure of DYRK1A/harmine complex[59] (PDB 3ANR) as a starting point. The IFD protocol modifies both the ligand and protein conformations to account for receptor flexibility. Within this protocol the protein-ligand complex conformations are ranked using the IFDScore, which is an empirical scoring function that combines Prime_Energy (the energy of the protein conformation), GlideScore (an approximation of the ligand binding free energy), and Glide_Ecoul (Coulombic interaction energy).[62] While no explicit water molecules are included in our starting model due to the uncertainty in positioning these molecules, GlideScore does include solvation terms that simulate the effects of solvent.[63] Glide docks explicit water molecules into the binding site for each energetically favorable ligand pose and employs empirical scoring terms that measure the exposure of various groups to the explicit waters. This explicit approach overcomes some of the limitations of continuum solvation models, particularly in the highly constrained environment of a binding site containing a bound ligand. Ligands and receptor were prepared using LigPrep and the Protein Preparation Wizard.[64] MM/GBSA binging energy calculations were carried out with Prime MM-GBSA using the VSGB 2.0 solvation model.[65] Figures were prepared using PyMOL 2.0 (Schrödinger, LLC).

DYRK1A Binding Assays: Compounds were tested for DYRK1A binding activity by a commercial kinase profiling services, Life Technologies which uses the FRET-based LanthaScreen® Eu Kinase Binding Assay[66]. Compounds were screened for DYRK1A activity at concentrations of 1000 nM and 300 nM in duplicates. The IC_{50} was determined by 10 point LanthaScreen® Eu Kinase Binding Assay[66] in duplicates.

B-cell proliferation assay: Human pancreatic islets were obtained from the NIH/NIDDK-supported Integrated Islet Distribution Program (IIDP) (https://iidp.coh.org). Islets were first dispersed with Accutase (Sigma, St. Louis, MO) onto coverslips as described earlier.[6] Dispersed islets were treated with vehicle (0.1% DMSO) or with harmine-related compounds in RPMI1640 complete medium for 96 hours. Then the cells were fixed and stained for insulin and Ki67.[6] Total insulin positive cells and cells double positive Ki67 and insulin positive cells were imaged and counted. Islets from 3-5 different adult donors were tested as descriebed in **Figure 3**, and at least 1000 beta cells cells were counted for human islet donor.

NFAT2 translocation assay: The immortalized R7T1 rat beta cell line was infected with aan adenovirus expressing NFAT2-GFP[6] for 48 hours, then the cells were treated with different compounds at 10 μM for another 24 hours. The cells were imaged and counted for the NFAT2-GFP nuclear translocation. At least 1000 cells were counted.

Kinome Scan Profile: Compounds were screened against 468 kinases at single concentration of 10 μM in duplicates at DiscoverX using their proprietary KINOMEscan® Assay.[67] The results for primary screen binding interactions are reported as '% DMSO Ctrl', where lower values indicate stronger affinity.

Synthetic Procedures:

7-Methoxy-2,9-dihydro-β-carbolin-1-one (1-4)

m-Anisidine (1.096 mL, 38.56 mmol) was dissolved in 15 mL of concentrated hydrochloric acid and, after cooling 15 mL of water was added to the solution. Sodium nitrite (2.74 g, 39.71 mmol) in 15mL of water was added dropwise to the cold suspension and stirred for 1 hour while maintaining the temperature below 10 ^{o}C. This solution was added to a cold solution of ethyl 3-carboxy-2-piperidone (7.0 g, 40.88 mmol) and potassium hydroxide (2.63 g, 47.01 mmol) in 20 mL of water which had been kept overnight at room temperature. The pH of the reaction mixture was adjusted to 4-5 by saturated aqueous solution of sodium acetate. The resultant mixture was stirred at room temperature for 5 hours. The yellow solid was filtered and washed with small amount of water and ethanol to give 6-methoxyphenylhydrazone 1-2 which was immediately taken to the next step. The phenylhydrazone 1-2 was refluxed in 25 mL of formic acid for 1 hour. The solution was neutralized with saturated aqueous solution of sodium carbonate and extracted with 100 mL of ethyl acetate three times. The organic layer was collected, dried over magnesium sulfate, filtered and solvent was rotary evaporated to give the desired tetrahydro-oxo-β-carboline 2-3. To a solution of Compound **1-3** in 60 mL of 1,4-dioxane was added DDQ (2.65 g, 11.7 mmol) in 40 mL 1,4-dioxane dropwise at 0 ^{o}C and stirred for 1 hour at room temperature. Upon completion of the reaction, 100 mL of water was added to the reaction. The product mixture was transferred to a separatory funnel and extracted with ethyl acetate (100 mL X 3) three times. The organic layer was washed with 0.1 N sodium hydroxide solution (50 mL X 3). The combined organic layer was then dried over magnesium sulfate, filtered and concentrated to provide the desired 7-methoxy-2,9-dihydro-β-carbolin-1-one **1-4** (1.91 g, 23% in 4 steps) as yellow solid. ^{1}H-NMR (600 MHz, CD_3OD): δ 7.85 (d, 1H, J = 9 Hz), 7.12 (d, 1H, J = 4.8 Hz), 7.06-7.08 (m, 2H), 6.86 (d, 1H, J = 6.6 Hz), 3.89 (s, 3H); ^{13}C-NMR (150 MHz, d_6-DMSO): δ159.40, 155.72,

140.74, 127.75, 125.12, 122.58, 116.40, 110.78, 99.85, 94.69, 55.61; HRMS (ESI): m/z [M + H]+ calcd for C12H11N2O2+: 215.0815, found: 215.0806.

1-Chloro-7-methoxy-9H-β-carboline (1-5):

A solution of 7-methoxy-2,9-dihydro-β-carbolin-1-one (1.80 g, 8.49 mmol) in $POCl_3$(20 mL) was stirred at 150 ^oC for 24 hours. The mixture was neutralized with the saturated aqueous solution of sodium carbonate. The solution was transferred to separatory funnel and extracted with ethyl acetate (50 mL X 3). The organic layer was collected, dried over magnesium sulfate, filtered and concentrated to provide the desired 1-Chloro-7-methoxy-9H-β-carboline **1-5** (1.56 g, 79%) as yellow solid. ^{1}H-NMR (600 MHz, $CDCl_3$): δ 8.31 (s, 1H), 8.19 (d, 1H, *J* = 5.4 Hz), 7.96 (d, 1H, *J* = 8.4 Hz), 7.78 (s, 1H, *J* = 5.4 Hz), 7.0 (s, 1H), 6.95 (m, 1H), 3.93 (s, 3H); ^{13}C-NMR (150 MHz, d_6-DMSO): δ161.14, 142.87, 138.10, 132.93, 132.83, 130.73, 123.44, 115.06, 114.39, 110.60, 95.28, 55.78; HRMS (ESI): m/z [M + H]+ calcd for C12H10ClN2O+: 233.0476, found: 233.0471. Purity >95%

General procedure for the synthesis of 1-amino-7-methoxy-9H-β-carboline (1-6)

A solution of 1-chloro-7-methoxy-9H-β-carboline (1 mmol) and amine (10 mmol) in a sealed pressure vessel was heated to 170 ^oC for 24 hour. Upon the completion of the reaction monitered by LCMS, the reaction mixture was concentrated and purified by flash column chromatography using DCM/MeOH as eluent to afford the desired 1-amino-7-methoxy-9H-β-carboline **1-6** as white solid.

1-(azetidin-1-yl)-7-methoxy-9H-β-carboline (1-6a)[53]

A screw-cap pressure vessel, equipped with a magnetic stir bar, was charged with 1-5 (50 mg, 0.21 mmol) RuPhos (1 mg, 1 mol %) and RuPhos precatalyst (P1) (1.75 mg, 1 mol %). The vial

was evacuated and backfilled with argon, and sealed with a Teflon screw cap. LiHMDS (1M in THF, 2.4 eq.) was added via syringe, followed by azetidine (0.25 mmol, 1.2 equiv.). The reaction mixture was heated at 90 ˚C for 96 h. Conversion for the reaction was low. The solution was allowed to cool to room temperature, then quenched by the addition of 1M HCl (1 mL), diluted with EtOAc and poured into sat. $NaHCO_3$. After extracting with EtOAc, the combined organic layers were washed with brine, dried over MgSO4, then concentrated and purified by flash column chromatography using MeOH/DCM (10/90) as eluent to afford compound 1-6a (6.5 mg, 31% based on 32 mg (64%), recovered starting material) as white solid. ^{1}H-NMR (600 MHz, $CDCl_3$): δ 7.98 (m, 1H), 7.90 (d, 1H, J = 9 Hz), 7.30 (m,1 H), 6.94 (m,1 H), 6.89 (d, 1H, J = 8.4 Hz), 4.38 (t, 4 H, J = 7.2 Hz), 3.90 (s, H), 2.52 (m, 2 H); ^{13}C-NMR (150 MHz, d_6-DMSO): δ 159.83, 149.05, 141.87, 136.84, 128.30, 123.52, 122.33, 115.48, 109.56, 106.39, 95.22, 55.61, 51.82, 17.42; HRMS (ESI): m/z [M + H]+ calcd for C15H16N3O+: 254.1288, found: 254.1284; Purity >95%

1-(Pyrrolidin-1-yl)-7-methoxy-9H-β-carboline (1-6b)

White solid. Yield 64%. ^{1}H-NMR (600 MHz, d_6-DMSO): δ 8.32 (s, 1H), 7.94 (d, 1H, J = 5.4 Hz), 7.89 (d, 1H, J = 8.4 Hz), 7.22 (d, 1H, J = 5.4 Hz), 6.93 (s, H), 6.88 (d, 1H, J = 8.4 Hz), 3.90 (m, 7H), 2.07 (s, 4 H); ^{13}C-NMR (150 MHz, d_6-DMSO): δ 159.64, 146.72, 141.52, 136.88, 128.60, 123.63, 122.09, 115.48, 109.43, 104.82, 95.28, 55.58, 48.39, 25.35; HRMS (ESI): m/z [M + H]+ calcd for C16H18N3O+: 268.1444, found: 268.1460; Purity >95%

1-(Piperidin-1-yl)-7-methoxy-9H-β-carboline (1-6c)

White solid. Yield 87%. ^{1}H-NMR (600 MHz, d_6-DMSO): δ 8.05 (d, 1H, J = 5.4 Hz), 7.90 (d, 1H, J =8.4 Hz), 7.48 (d, 1H, J = 4.8 Hz), 7.04 (s, 1H), 6.90 (m, 1H), 3.90 (s, 3H), 3.48 (broad s, 4H), 1.84 (broad s, 4H), 1.70 (m, 2H); ^{13}C-NMR (150 MHz, d_6-DMSO): δ159.98, 149.23,

141.74, 136.57, 129.05, 126.62, 122.33, 115.66, 109.43, 108.75, 95.20, 55.60, 49.92, 26.09, 24.82; HRMS (ESI): m/z [M + H]+ calcd for C17H20N3O+: 282.1601, found: 282.1590; Purity >95%

1-(2-Phenylpyrrolidin-1-yl)-7-methoxy-9H-β-carboline (1-6d)

Brown solid. Yield 80%. ^{1}H-NMR (600 MHz, $CDCl_3$): δ 7.98 (d, 1H, *J* = 5.4 Hz), 7.82 (d, 1H, *J* = 8.4 Hz), 7.61 (s, 1H), 7.51 (d, 2H, *J* = 7.2 Hz), 7.44 (t, 2H, *J* = 7.8 Hz), 7.34 (t, 2H, *J* = 7.2 Hz), 7.24 (d, 1H, *J* = 5.4 Hz), 6.79 (m, 1H), 6.49 (d, 1H, *J* = 1.8 Hz), 5.48 (d, 1H, *J* = 8.4 Hz), 4.06 (m, 1H), 4.01 (m, 1H), 3.82 (s, 3 H), 2.46 (m, 1H), 2.04 (m, 3H); ^{13}C-NMR (150 MHz, d_6-DMSO): δ 159.75, 146.24, 145.92, 141.60, 136.78, 128.85, 128.39, 126.45, 126.28, 124.43, 122.15, 115.49, 109.43, 105.63, 95.25, 61.35, 55.62, 50.48, 24.53; HRMS (ESI): m/z [M + H]+ calcd for C22H22N3O+: 344.1757, found: 344.1761; Purity >95%

1-(3-Phenylpyrrolidin-1-yl)-7-methoxy-9H-β-carboline (1-6e)

Brown solid. Yield 59%. ^{1}H-NMR (600 MHz, d_6-DMSO): δ 8.17 (s, 1H), 7.98 (d, 1H, *J* = 6 Hz), 7.91 (d, 1H, *J* = 9 Hz), 7.37 (m, 4H), 7.27 (m, 2H), 6.91 (s, 1H), 6.88 (d, 2H, *J* = 9 Hz), 4.33 (t, (d, 1H, *J* = 8.4 Hz), 4.09 (m, 1H), 4.01 (m, 1H), 3.94 (t, 1H, *J* = 8.4 Hz), 3.81 (s, 3H), 3.60 (m, 1H), 2.49 (m, 1H), 2.24 (m, 1H); ^{13}C-NMR (150 MHz, $CDCl_3$): δ161.19, 143.50, 141.54, 139.47, 130.03, 128.60, 126.97, 121.83, 114.64, 112.61, 104.69, 95.30, 55.53, 50.12, 43.47, 32.24; HRMS (ESI): m/z [M + H]+ calcd for C22H22N3O+: 344.1757, found: 344.1750; Purity >95%

1-(2-Benzylpyrrolidin-1-yl)-7-methoxy-9H-β-carboline (1-6f)

Brown solid. Yield 65%. ^{1}H-NMR (600 MHz, $CDCl_3$): δ 8.05 (d, 1H, *J* = 5.4 Hz), 7.91 (d, 2H, *J* = 9 Hz), 7.28 (m, 5H), 6.88 (m, 2H), 4.68 (s, 1H), 3.90 (m, 5H), 3.22 (m,1H), 2.79 (m, 1H), 1.97 (m, 3H), 1.84 (m, 1H); ^{13}C-NMR (150 MHz, $CDCl_3$): δ160.66, 142.04, 138.44, 129.63, 128.26,

126.31, 121.94, 115.48, 110.80, 105.33, 94.95, 60.45, 55.54, 50.04, 39.36, 29.77, 23.65; HRMS (ESI): m/z [M + H]+ calcd for C23H24N3O+: 358.1914, found: 358.1900; Purity >95%

1-(3-Benzylpyrrolidin-1-yl)-7-methoxy-9H-β-carboline (1-6g)

Brown solid. Yield 71%. ^{1}H-NMR (600 MHz, $CDCl_3$): δ 8.14 (s, 1H), 7.96 (d, 1H, *J* = 5.4 Hz), 7.90 (d, 2H, *J* = 9 Hz), 7.32 (m, 2H), 7.25 (m, 4H), 6.93 (s,1H), 6.87 (d, 1H, *J* = 5.4 Hz), 4.01 (m, 2H), 3.90 (m, 4H), 1.08 (t, 1H, *J* = 9 Hz), 2.87 (m, 1H), 2.81 (m, 1H), 2.69 (m,1H), 2.17 (m, 1H), 1.83 (m, 1H); ^{13}C-NMR (150 MHz, d_6-DMSO): δ159.62, 146.71, 141.52, 141.15, 137.03, 129.15, 128.76, 126.38, 123.56, 122.08, 115.49, 109.41, 104.81, 95.29, 55.58, 53.80, 47.95, 31.18; HRMS (ESI): m/z [M + H]+ calcd for C23H24N3O+: 358.1914, found: 358.1901; Purity >95%

1-(2-(2-Chlorophenyl)pyrrolidin-1-yl)-7-methoxy-9H-β-carboline (1-6h)

Yellow solid. Yield 77%. ^{1}H-NMR (600 MHz, $CDCl_3$): δ 7.98 (d, 1H, *J* = 5.4 Hz), 7.83 (d, 1H, *J* = 8.4 Hz), 7.52 (m, 3H), 7.25 (m, 3H), 6.80 (m, 1H), 6.59 (d, 1H, *J* = 2.4 Hz), 5.80 (d, 1H, *J* = 8.4 Hz), 4.10 (m, 2H), 3.84 (s, 3 H), 2.54 (m, 1H), 2.04 (m, 3H); ^{13}C-NMR (150 MHz, d_6-DMSO): δ159.82, 145.77, 142.92, 141.72, 136.88, 131.91, 129.73, 129.08, 128.20, 127.30, 124.39, 122.17, 115.53, 109.47, 105.73, 95.33, 59.41, 55.62, 50.31, 32.65, 24.60; HRMS (ESI): m/z [M + H]+ calcd for C22H21ClN3O+: 378.1368, found: 378.1366; Purity >95%

1-(2-(3-Chlorophenyl)pyrrolidin-1-yl)-7-methoxy-9H-β-carboline (1-6i)

Yellow solid. Yield 68%. ^{1}H-NMR (600 MHz, $CDCl_3$): δ 7.96 (d, 1H, *J* = 5.4 Hz), 7.86 (d, 1H, *J* = 8.4 Hz), 7.69 (s, 1H), 7.39 (m, 1H), 7.37 (d, 1H, *J* = 7.8 Hz), 7.33 (t, 1H, *J* = 7.2 Hz), 7.28 (m, 2H), 6.83 (m, 1H), 6.65 (m, 1H), 5.51 (d, 1H, *J* = 8.4 Hz), 4.07 (m, 2H), 3.84 (s, 3H), 2.46 (m, 1H), 2.04 (m, 3H); ^{13}C-NMR (150 MHz, d_6-DMSO): δ159.84, 148.77, 146.08, 141.72, 136.73, 133.18, 130.33, 129.03, 126.48, 125.14, 122.20, 115.53, 109.51, 105.94, 95.30, 61.51, 55.62,

50.60, 35.23, 24.75; HRMS (ESI): m/z [M + H]+ calcd for C22H21ClN3O+: 378.1368, found: 378.1377; Purity >95%

1-(2-(4-Chlorophenyl)pyrrolidin-1-yl)-7-methoxy-9H-β-carboline (1-6j)

Yellow solid. Yield 43%. ^{1}H-NMR (600 MHz, $CDCl_3$): δ 7.97 (d, 1H, *J* = 5.4 Hz), 7.84 (d, 1H, *J* = 8.4 Hz), 7.66 (s, 1H), 7.44 (d, 2H, *J* = 8.4 Hz), 7.38 (d, 2H, *J* = 8.4 Hz), 7.27 (m, 1H), 6.83 (m, 1H), 6.64 (m, 1H), 5.50 (d, 1H, *J* = 8.4 Hz), 4.06 (m, 2H), 3.84 (s, 3H), 2.47 (m, 1H), 2.04 (m, 3H); ^{13}C-NMR (150 MHz, d_6-DMSO): δ159.80, 146.08, 144.98, 141.66, 136.78, 130.85, 128.95, 128.33, 124.47, 122.16, 115.51, 109.46, 105.81, 95.28, 60.99, 55.61, 50.49, 35.26, 24.63; HRMS (ESI): m/z [M + H]+ calcd for C22H21ClN3O+: 378.1368, found: 378.1365; Purity >95%

β-Carboline-N-oxide (2-1)

To a solution of harmine (500 mg, 2.35 mmol) in 8 mL of chloroform was added 3-chloroperoxybenzoic acid (1.22 g, 7.05 mmol) and refluxed for 24 hours. The reaction mixture was concentrated and purified by flash chromatography using DCM/MeOH as eluent to give the desired product β-carboline-N-oxide **2-1** (255 mg, 47%) as white solid. ^{1}H-NMR (600 MHz, d_6-DMSO): δ 11.60 (s, 1H), 8.04 (d, 1H, *J* = 6.6 Hz), 8.00 (d, 1H, *J* = 8.4 Hz), 7.86 (d, 1H, *J* = 6.6 Hz), 6.97 (s, 1H), 6.85 (m, 1H), 3.85 (s, 3H), 2.61 (s, 3H); ^{13}C-NMR (150 MHz, d_6-DMSO): δ159.82, 143.39, 136.55, 132.79, 131.31, 122.35, 119.13, 115.62, 113.67, 109.57, 95.18, 55.78, 13.00; HRMS (ESI): m/z [M + H]+ calcd for C13H13N2O2+: 229.0972, found: 229.0962; Purity >95%

1-Hydroxymethyl-7-methoxy-9H-β-carboline (2-2)

Trifluoroacetic anhydride (2.20 mL, 15.87 mmol) was added to a stirred mixture of **β-carboline-N-oxide (2-1)** (724 mg, 3.17 mmol) and CH_2Cl_2 (20 mL) at 0 ^{o}C. After being stirred for 30 min, the mixture was refluxed 12 h. Upon completion of the reaction monitored by TLC, the mixture was concentrated and purified by flash column chromatography using DCM/MeOH as eluent to

afford the 1-hydroxymethyl-7-methoxy-9H-β-carboline **2-2** (358 mg, 49%) as white solid. ^{1}H-NMR (600 MHz, CD_3OD): δ 8.39 (d, 1H, *J* = 6 Hz), 8.27 (d, 1H, *J* = 6 Hz), 8.22 (d, 1H, *J* = 9 Hz), 7.15 (s, 1H), 7.06 (m, 1H), 5.31 (s, 2H), 3.96 (s, 3 H); ^{13}C-NMR (150 MHz, d_6-DMSO): δ163.11, 145.98, 140.04, 133.09, 131.95, 129.49, 124.80, 115.17, 113.83, 112.77, 94.96, 58.27, 56.10; HRMS (ESI): m/z [M + H]+ calcd for C13H13N2O2+: 229.0972, found: 229.0967; Purity >95%

3-Bromo-2-hydroxyimino-propionic acid ethyl ester (2-3)[56]

Hydroxylamine hydrochloride (1.81 g, 25.63 mmol) was added to a stirred solution of ethyl bromopyruvate (5.01 g, 25.63 mmol) in chloroform (50 mL) and methanol (70 mL) at room temperature. The reaction mixture was stirred for 24 hours and concentrated under reduced pressure. The crude was dissolved in dichloromethane (300 mL) and washed with 0.1 N of hydrochloric acid and brine. The organic layer was collected, dried over magnesium sulfate, filtered, and concentrated to give 3-bromo-2-hydroxyimino-propionic acid ethyl ester **2-3** (4.36 g, 81%) as white solid. ^{1}H-NMR (600 MHz, $CDCl_3$): δ 10.08 (bs, 1H), 4.38 (q, J=7.2 Hz, 2H), 4.27 (s, 2H), 1.39 (t, J=7.2 Hz, 3H); ESI: m/z [M + H]+ 209.97.

3-(6-Methoxy-1H-indol-3- yl)-propionic acid ethyl ester (2-4)

A solution of 3-bromo-2-hydroxyimino-propionic acid ethyl ester **2-3** (1.75 g, 8.35 mmol) in CH_2Cl_2 (20 mL) was slowly added dropwise to a stirring mixture of 6-methoxyindole (1.23 g, 8.35 mmol) and Na_2CO_3 (4.86 g, 45.92 mmol) in CH_2Cl_2 (20 mL) at room temperature. The mixture was stirred for 48 h, filtered through Celite, concentrated, and purified by flash column chromatography using ethyl acetate\Hexanes as eluent to give 3-(6-methoxy-1H-indol-3- yl)-propionic acid ethyl ester **2-4** (800 mg, 34%) as white solid.^{1}H-NMR (600 MHz, d_6-DMSO): δ

7.91 (s, 1 H), 7.65 (d, 1 H, *J* = 12 Hz), 7.00 (s, 1 H), 6.81 (m, 1 H), 4.05 (s, 2 H), 4.26 (m, 2 H), 1.31 (t, 3 H, *J* = 6 Hz); ^{13}C-NMR (150 MHz, d_6-DMSO): δ164.20, 155.94, 150.66, 137.05, 122.75, 121.74, 119.65, 109.07, 94.78, 61.15, 55.53, 20.47, 14.36; HRMS (ESI): m/z [M + H]+ calcd for C14H17N2O4+: 227.1183, found: 227.1192; Purity >95%

2-Amino-3-(6-methoxy-1H-indol-3-yl)-propionic acid ethyl ester (2-5)

Zn dust (3.11 g, 47.62 mmol) was added portion wise to a stirred solution of **2-4** (1.64 g, 5.95 mmol) in acetic acid (20 mL) over 30 min. After addition, the mixture was stirred overnight at room temperature. After completion of the reaction monitored by LCMS, the mixture was filtered through Celite, washed with acetic acid (20 mL) and concentrated. The residue was neutralized with saturated aqueous solution of sodium bicarbonate and extracted with ethyl acetate (30 mLX3). Organic layers were collected, dried over magnesium sulfate, filtered, concentrated to get 2-amino-3-(6-methoxy-1H-indol-3-yl)-propionic acid ethyl ester **2-5** (1.5 g, 96%) as white solid. ^{1}H-NMR (600 MHz, d_6-DMSO): δ 10.64 (s, 1H), 7.35 (d, 1H, *J* = 8.4 Hz), 6.96 (s, 1H), 6.82 (s, 1H), 6.63 (m, 1H), 3.99 (m, 2H), 3.74 (s, 3H), 3.56 (m, 1H), 2.86-2.97 (m, 2H), 1.90 (s, 1H), 1.10 (t, 3H, *J* = 7.2 Hz); ^{13}C-NMR (150 MHz, d_6-DMSO): δ155.85, 137.21, 122.60, 119.31, 110.32, 108.92, 94.81, 60.28, 55.60, 31.29, 14.42; HRMS (ESI): m/z [M + H]+ calcd for C14H19N2O3+: 263.1390, found: 263.1399; Purity >95%

Ethyl 1-methyl-7-methoxy-9H-pyrido[3,4-b]indole-3-carboxylate (2-7)

To the mixture of **2-5** (1 g, 3.81 mmol) and acetaldehyde (40% in water, 0.46 mL, 4.19 mmol) in 15 mL of dichloromethane, 0.4 mL of trifluoroacetic acid was added drops wise at 0 ^{o}C. Then, reaction mixture was stirred at room temperature for 12 h. After completion of reaction as monitored by TLC, the reaction mixture was transferred to separatory funnel and washed with 50 mL of saturated sodium bicarbonate solution and brine. Organic layer was dried over anhydrous

magnesium sulfate, filtered and concentrated under vacuum to get **2-6** as a white solid which was taken to next step without purification. A mixture of **2-6** (1.04 g, 3.81 mmol) and sulfur (248 mg, 7.63 mmol) in xylene (150 mL) was heated at reflux for 12 h. Then the mixture was concentrated under reduced pressure and purified by flash column chromatography using DCM\/MeOH as eluent to afford Ethyl 1-Methyl-7-methoxy-9H-pyrido[3,4-b]indole-3-carboxylate **2-7** (755 mg, 75%) as brown solid. ^{1}H-NMR (600 MHz, d_6-DMSO): δ 11.49 (s, 1 H), 9.10 (s, 1 H), 8.62 (d, 1 H, J = 8.4 Hz), 7.54 (s, 1 H), 7.38 (m, 1 H), 4.84 (q, 2 H, J = 7.2 Hz), 4.33 (s, 3 H), 3.22 (s, 3 H), 1.82 (t, 1 H, J = 6.6 Hz); ^{13}C-NMR (150 MHz, d_6-Acetone): δ166.31, 161.50, 143.09, 141.66, 137.98, 136.84, 128.25, 123.03, 116.01, 115.32, 110.61, 95.33, 60.72, 55.36, 19.94, 14.30 ; HRMS (ESI): m/z [M + H]+ calcd for C16H17N2O3+: 185.1234, found: 285.1237; Purity >95%

(1-Methyl-7-methoxy-9H-pyrido[3,4-b]indol-3-yl)methanol (2-8)

To a solution of ester **2-7** (160 mg, 0.56 mmol) in THF (15 mL) was added LiAlH4 (44 mg, 1.17 mmol) in portions at 0 °C, and then the mixture was stirred overnight at room temperature. Then the reaction was quenched by water and stirred at room temperature for 2 h, the slurry was filtered, the cake was washed with dichloromethane, the filtrate was concentrated to afford **2-8** (135 mg, 91%) as white solid. ^{1}H-NMR (600 MHz, d_6-DMSO): δ 11.31 (s, 1H), 8.05 (d, 1H, J = 8.4 Hz), 7.83 (s, 1H), 6.98 (s, 1H), 6.82 (d, 1H, J = 8.4 Hz), 5.25 (s, 1H), 4.64 (d, 2H, J = 5.4 Hz) 3.86 (s, 3 H), 2.68 (s, 3 H); ^{13}C-NMR (150 MHz, d_6-DMSO): δ160.43, 150.39, 142.71, 140.30, 133.87, 128.53, 122.95, 115.41, 109.31, 108.51, 94.99, 65.02, 55.71, 20.56; HRMS (ESI): m/z [M + H]+ calcd for C14H15N2O2+: 243.1128, found: 243.1131; Purity >95%

1,3-dimethyl-7-methoxy-9H-β-carboline (2-9)[58]

To a solution of **2-8** (20 mg, 0.082 mmol) and $PdCl_2$ (4 mg, 0.016 mmol) in EtOH (1 mL) was added Et_3SiH (0.201 mL, 1.28 mmol) and the mixture was stirred at 90 ^oC for 5 hours. Upon completion of reaction monitored by TLC, catalyst was filtered over celite and the filetrate was evaporated. The crude reaction mixture was purified by column chromatography using ethyl acetate as eluent to afford **2-9** (5 mg, 27%) as white solid. ^{1}H-NMR (600 MHz, d_6-DMSO): δ 8.01 (d, 1H, J = 7.8 Hz), 7.66 (s, 1H), 6.96 (s, 1H), 6.81 (d, 1H, J = 7.8 Hz), 3.86 (s, 3H), 2.68 (s, 3 H), 2.53 (s, 3 H); HRMS (ESI): m/z [M + H]+ calcd for C14H15N2O+: 227.1179, found: 227.1169; Purity >95%

1-acetyl-7-methoxy-9H-β-carboline (3-2)

To the mixture of 6-methoxytryptamine (300 mg, 1.57 mmol) and pyruvicaldehyde (45% in water, 0.34 mL, 1.89 mmol) in 6 mL of dichloromethane, 0.157 mL of trifluoroacetic acid was added drops wise at 0 ^oC. Then, reaction mixture was stirred at room temperature for 12 h. After completion of reaction as monitored by TLC, the reaction mixture was transferred to separatory funnel and washed with 50 mL of saturated sodium bicarbonate solution and brine. Organic layer was dried over anhydrous magnesium sulfate, filtered and concentrated under vacuum to get **3-1** as yellow solid which was taken to next step without purification. A mixture of **3-1** (1.57 mmol) and $KMnO_4$ (744 mg, 4.71 mmol) in THF (5 mL) was stirred at room temperature for 12 h. Then the mixture was concentrated under reduced pressure and purified by flash column chromatography using ethyl acetate as eluent to afford 1-acetyl-7-methoxy-9H-β-carboline **3-2** (60 mg, 16%) as brown solid. ^{1}H-NMR (600 MHz, d_6-DMSO): δ 11.75 (s, 1 H), 8.45 (d, 1 H, J = 5.4 Hz), 8.30 (d, 1 H, J = 4.8 Hz), 8.16 (d, 1 H, J = 8.4 Hz), 7.31 (m, 1 H), 6.92 (m, 1 H), 3.86 (s, 3 H), 2.77 (s, 3 H); ^{13}C-NMR (150 MHz, d_6-DMSO): δ 201.88, 161.20, 144.06, 138.14,

135.78, 134.69, 131.58, 123.18, 118.88, 113.89, 110.24, 96.40, 55.76, 26.32; HRMS (ESI): m/z [M + H]+ calcd for C14H13N2O2+: 241.0972, found: 241.0966; Purity >95%

1-(1-hydroxyethyl)-7-methoxy-9H-β-carboline (3-3)

To a solution of **3-2** (12 mg, 0.05 mmol) in MeOH (2 mL) was added $NaBH_4$ (4 mg, 0.1 mmol) and the mixture was stirred overnight at room temperature. Then the reaction was quenched by water, transferred to separatory funnel and extracted with ethyl acetate. Organic layer was collected, dried over magnesium sulfate, filtered and rotary evaporated to get the desired compound **3-3** (6 mg, 49%) as yellow solid. ^{1}H-NMR (600 MHz, d_6-DMSO): δ 11.09 (s, 1 H), 8.17 (d, 1 H, J = 4.8 Hz), 8.05 (d, 1 H, J = 8.4 Hz), 7.86 (d, 1 H, J = 4.8 Hz), 7.17 (m, 1 H), 6.82 (m, 1 H), 5.67 (d, 1 H, J = 4.8 Hz), 5.16 (m, 1 H), 3.85 (s, 3 H), 1.53 (d, 3 H, J = 6 Hz); ^{13}C-NMR (150 MHz, d_6-DMSO): δ 160.46, 148.37, 142.56, 137.25, 132.78, 128.93, 122.66, 114.66, 113.15, 109.32, 95.46, 69.59, 55.67, 23.36; HRMS (ESI): m/z [M + H]+ calcd for C14H15N2O2+: 243.1128, found: 243.1131; Purity >95%

ASSOCIATED CONTENT

Supporting Information. DYRK1A binding curves, spectral data (PDF) and full kinome scans of harmine, compound **2-2** and **2-8**, Molecular Formula Strings are available free of charge via internet at http://pubs.acs.org.

AUTHOR INFORMATION

Corresponding Author

Robert J. DeVita. E-mail: robert.devita@mssm.edu. Phone: 212-659-5542;

Author Contributions

The manuscript was written through contributions of all authors. All authors have given approval to the final version of the manuscript.

Funding Sources

K.K., P.W., R.J.D. and A.F.S. were supported in part by NIH grant by NIDDK R01DK DK105015-01-A1, UC4 DK104211, P-30 DK 020541, JDRF 2-SRA-2017 514-S-B.

K.K. and R.J.D. were supported in part by Icahn School of Medicine Seed Fund 0285-3980. This work was supported in part through the computational resources and staff expertise provided by Scientific Computing at the Icahn School of Medicine at Mount Sinai, the NIDDK-supported Einstein-Sinai Diabetes Research Center (E-S DRC) and the NIDDK Human Ilseet Research Network.

ABBREVIATIONS

DYRK1A, The Dual-Specificity Tyrosine Phosphorylation-Regulated Kinase 1A; DS, Down syndrome; AD, Alzheimer's disease; NFAT, nuclear factor of activated T cells; EGCg, Epigallocatechin gallate; INDY, inhibitor of DYRK1A; FINDY, Folding intermediate inhibitor of DYRK1A; DANDY, diaryl azaindole inhibitor of DYRK1A; CNS, central nervous system; FRET, Fluorescence resonance energy transfer; SAR, structure activity relationship; TLC, thin layer chromatography.

REFERENCES:

1. Becker, W.; Soppa, U.; Tejedor, F. J., DYRK1A: A potential drug target for multiple down syndrome neuropathologies. *CNS Neurol. Disord.: Drug Targets* **2014,** *13* (1), 26-33.
2. Wegiel, J.; Gong, C.-X.; Hwang, Y.-W., The role of DYRK1A in neurodegenerative diseases. *FEBS J.* **2011,** *278* (2), 236-245.
3. Smith, B.; Medda, F.; Gokhale, V.; Dunckley, T.; Hulme, C., Recent advances in the design, synthesis, and biological evaluation of selective DYRK1A inhibitors: A new avenue for a disease modifying treatment of alzheimer's? *ACS Chem. Neurosci.* **2012,** *3* (11), 857-872.
4. Ionescu, A.; Dufrasne, F.; Gelbcke, M.; Jabin, I.; Kiss, R.; Lamoral-Theys, D., DYRK1A kinase inhibitors with emphasis on cancer. *Mini-Rev. Med. Chem.* **2012,** *12* (13), 1315-1329.
5. Fernandez-Martinez, P.; Zahonero, C.; Sanchez-Gomez, P., DYRK1A: the double-edged kinase as a protagonist in cell growth and tumorigenesis. *Mol. Cell. Oncol.* **2015**, e970048/1-e970048/11.
6. Wang, P.; Alvarez-Perez, J.-C.; Felsenfeld, D. P.; Liu, H.; Sivendran, S.; Bender, A.; Kumar, A.; Sanchez, R.; Scott, D. K.; Garcia-Ocana, A.; Stewart, A. F., A high-throughput chemical screen reveals that harmine-mediated inhibition of DYRK1A increases human pancreatic beta cell replication. *Nat. Med.* **2015,** *21* (4), 383-388.
7. Shen, W.; Taylor, B.; Jin, Q.; Nguyen-Tran, V.; Meeusen, S.; Zhang, Y.-Q.; Kamireddy, A.; Swafford, A.; Powers, A. F.; Walker, J.; Lamb, J.; Bursalaya, B.; DiDonato, M.; Harb, G.; Qiu, M.; Filippi, C. M.; Deaton, L.; Turk, C. N.; Suarez-Pinzon, W. L.; Liu, Y.; Hao, X.; Mo, T.; Yan, S.; Li, J.; Herman, A. E.; Hering, B. J.; Wu, T.; Seidel, H. M.; McNamara,

P.; Glynne, R.; Laffitte, B., Inhibition of DYRK1A and GSK3B induces human β-cell proliferation. *Nat. Commun.* **2015,** *6*, 8372-8382.

8. Rachdi, L.; Kariyawasam, D.; Aiello, V.; Herault, Y.; Janel, N.; Delabar, J.-M.; Polak, M.; Scharfmann, R., Dyrk1A induces pancreatic β cell mass expansion and improves glucose tolerance. *Cell Cycle* **2014,** *13* (14), 2221-2229.
9. Dirice, E.; Walpita, D.; Vetere, A.; Meier, B. C.; Kahraman, S.; Hu, J.; Dancik, V.; Burns, S. M.; Gilbert, T. J.; Olson, D. E.; Clemons, P. A.; Kulkarni, R. N.; Wagner, B. K., Inhibition of DYRK1A stimulates human beta-cell proliferation. *Diabetes* **2016,** *65* (6), 1660-1671.
10. Becker, W.; Sippl, W., Activation, regulation, and inhibition of DYRK1A. *FEBS J.* **2011,** *278* (2), 246-256.
11. Guedj, F.; Sebrie, C.; Rivals, I.; Ledru, A.; Paly, E.; Bizot, J. C.; Smith, D.; Rubin, E.; Gillet, B.; Arbones, M.; Delabar, J. M., Green tea polyphenols rescue of brain defects induced by overexpression of DYRK1A. *PLoS One* **2009,** *4* (2), e4606
12. Bain, J.; McLauchlan, H.; Elliott, M.; Cohen, P., The specificities of protein kinase inhibitors: an update. *Biochem. J.* **2003,** *371* (1), 199-204.
13. Tahtouh, T.; Elkins, J. M.; Filippakopoulos, P.; Soundararajan, M.; Burgy, G.; Durieu, E.; Cochet, C.; Schmid, R. S.; Lo, D. C.; Delhommel, F.; Oberholzer, A. E.; Pearl, L. H.; Carreaux, F.; Bazureau, J.-P.; Knapp, S.; Meijer, L., Selectivity, cocrystal structures, and neuroprotective properties of leucettines, a family of protein kinase inhibitors derived from the marine sponge alkaloid leucettamine B. *J. Med. Chem.* **2012,** *55* (21), 9312-9330.
14. Naert, G.; Ferre, V.; Meunier, J.; Keller, E.; Malmstrom, S.; Givalois, L.; Carreaux, F.; Bazureau, J.-P.; Maurice, T., Leucettine L41, a DYRK1A-preferential DYRKs/CLKs

inhibitor, prevents memory impairments and neurotoxicity induced by oligomeric Aβ25-35 peptide administration in mice. *Eur. Neuropsychopharmacol.* **2015,** *25* (11), 2170-2182.

15. Cozza, G.; Mazzorana, M.; Papinutto, E.; Bain, J.; Elliott, M.; di Maira, G.; Gianoncelli, A.; Pagano, M. A.; Sarno, S.; Ruzzene, M.; Battistutta, R.; Meggio, F.; Moro, S.; Zagotto, G.; Pinna, L. A., Quinalizarin as a potent, selective and cell-permeable inhibitor of protein kinase CK2. *Biochem. J.* **2009,** *421* (3), 387-395.
16. Ahmadu, A.; Abdulkarim, A.; Grougnet, R.; Myrianthopoulos, V.; Tillequin, F.; Magiatis, P.; Skaltsounis, A.-L., Two new peltogynoids from Acacia nilotica Delile with kinase inhibitory activity. *Planta Med.* **2010,** *76* (5), 458-460.
17. Sarno, S.; Mazzorana, M.; Traynor, R.; Ruzzene, M.; Cozza, G.; Pagano, M. A.; Meggio, F.; Zagotto, G.; Battistutta, R.; Pinna, L. A., Structural features underlying the selectivity of the kinase inhibitors NBC and dNBC: role of a nitro group that discriminates between CK2 and DYRK1A. *Cell. Mol. Life Sci.* **2012,** *69* (3), 449-460.
18. Sanchez, C.; Salas, A. P.; Brana, A. F.; Palomino, M.; Pineda-Lucena, A.; Carbajo, R. J.; Mendez, C.; Moris, F.; Salas, J. A., Generation of potent and selective kinase inhibitors by combinatorial biosynthesis of glycosylated indolocarbazoles. *Chem. Commun.* **2009,** (27), 4118-4120.
19. Ogawa, Y.; Nonaka, Y.; Goto, T.; Ohnishi, E.; Hiramatsu, T.; Kii, I.; Yoshida, M.; Ikura, T.; Onogi, H.; Shibuya, H.; Hosoya, T.; Ito, N.; Hagiwara, M., Development of a novel selective inhibitor of the Down syndrome-related kinase Dyrk1A. *Nat. Commun.* **2010,** *1*, Oga1/1-Oga1/9,SOga1/1-SOga1/19.
20. Gourdain, S.; Dairou, J.; Denhez, C.; Bui, L. C.; Rodrigues-Lima, F.; Janel, N.; Delabar, J. M.; Cariou, K.; Dodd, R. H., Development of DANDYs, new 3,5-Diaryl-7-azaindoles

demonstrating potent DYRK1A kinase inhibitory activity. *J. Med. Chem.* **2013,** *56* (23), 9569-9585.

21. Kii, I.; Sumida, Y.; Goto, T.; Sonamoto, R.; Okuno, Y.; Yoshida, S.; Kato-Sumida, T.; Koike, Y.; Abe, M.; Nonaka, Y.; Ikura, T.; Ito, N.; Shibuya, H.; Hosoya, T.; Hagiwara, M., Selective inhibition of the kinase DYRK1A by targeting its folding process. *Nat. Commun.* **2016,** *7*, 11391-11404.
22. Koo, K. A.; Kim, N. D.; Chon, Y. S.; Jung, M.-S.; Lee, B.-J.; Kim, J. H.; Song, W.-J., QSAR analysis of pyrazolidine-3,5-diones derivatives as Dyrk1A inhibitors. *Bioorg. Med. Chem. Lett.* **2009,** *19* (8), 2324-2328.
23. Kim, N. D.; Yoon, J.; Kim, J. H.; Lee, J. T.; Chon, Y. S.; Hwang, M.-K.; Ha, I.; Song, W.-J., Putative therapeutic agents for the learning and memory deficits of people with Down syndrome. *Bioorg. Med. Chem. Lett.* **2006,** *16* (14), 3772-3776.
24. Rosenthal, A. S.; Tanega, C.; Shen, M.; Mott, B. T.; Bougie, J. M.; Nguyen, D.-T.; Misteli, T.; Auld, D. S.; Maloney, D. J.; Thomas, C. J., Potent and selective small molecule inhibitors of specific isoforms of Cdc2-like kinases (Clk) and dual specificity tyrosine-phosphorylation-regulated kinases (Dyrk). *Bioorg. Med. Chem. Lett.* **2011,** *21* (10), 3152-3158.
25. Giraud, F.; Alves, G.; Debiton, E.; Nauton, L.; Thery, V.; Durieu, E.; Ferandin, Y.; Lozach, O.; Meijer, L.; Anizon, F.; Pereira, E.; Moreau, P., Synthesis, protein kinase inhibitory potencies, and in vitro antiproliferative activities of meridianin derivatives. *J. Med. Chem.* **2011,** *54* (13), 4474-4489.
26. Echalier, A.; Bettayeb, K.; Ferandin, Y.; Lozach, O.; Clelment, M.; Valette, A.; Liger, F.; Marquet, B.; Morris, J. C.; Endicott, J. A.; Joseph, B.; Meijer, L., Meriolins (3-(Pyrimidin-

4-yl)-7-azaindoles): Synthesis, kinase inhibitory activity, cellular effects, and structure of a CDK2/Cyclin A/Meriolin complex. *J. Med. Chem.* **2008,** *51* (4), 737-751.

27. Akue-Gedu, R.; Debiton, E.; Ferandin, Y.; Meijer, L.; Prudhomme, M.; Anizon, F.; Moreau, P., Synthesis and biological activities of aminopyrimidyl-indoles structurally related to meridianins. *Bioorg. Med. Chem.* **2009,** *17* (13), 4420-4424.
28. Kassis, P.; Brzeszcz, J.; Beneteau, V.; Lozach, O.; Meijer, L.; Le Guevel, R.; Guillouzo, C.; Lewinski, K.; Bourg, S.; Colliandre, L.; Routier, S.; Merour, J.-Y., Synthesis and biological evaluation of new 3-(6-hydroxyindol-2-yl)-5-(Phenyl) pyridine or pyrazine V-Shaped molecules as kinase inhibitors and cytotoxic agents. *Eur. J. Med. Chem.* **2011,** *46* (11), 5416-5434.
29. Neagoie, C.; Vedrenne, E.; Buron, F.; Merour, J.-Y.; Rosca, S.; Bourg, S.; Lozach, O.; Meijer, L.; Baldeyrou, B.; Lansiaux, A.; Routier, S., Synthesis of chromeno[3,4-b]indoles as Lamellarin D analogues : A novel DYRK1A inhibitor class. *Eur. J. Med. Chem.* **2012,** *49*, 379-396.
30. Falke, H.; Chaikuad, A.; Becker, A.; Loaec, N.; Lozach, O.; Abu Jhaisha, S.; Becker, W.; Jones, P. G.; Preu, L.; Baumann, K.; Knapp, S.; Meijer, L.; Kunick, C., 10-Iodo-11H-indolo[3,2-c]quinoline-6-carboxylic acids are selective inhibitors of DYRK1A. *J. Med. Chem.* **2015,** *58* (7), 3131-3143.
31. Foucourt, A.; Heou, D.; Dubouilh-Benard, C.; Desire, L.; Casagrande, A.-S.; Leblond, B.; Loaec, N.; Meijer, L.; Besson, T., Design and synthesis of thiazolo[5,4-f]quinazolines as DYRK1A inhibitors, part I. *Molecules* **2014,** *19* (10), 15546-15571, 26 pp.
32. Coutadeur, S.; Benyamine, H.; Delalonde, L.; de Oliveira, C.; Leblond, B.; Foucourt, A.; Besson, T.; Casagrande, A.-S.; Taverne, T.; Girard, A.; Pando, M. P.; Desire, L., A novel

DYRK1A (Dual specificity tyrosine phosphorylation-regulated kinase 1A) inhibitor for the treatment of Alzheimer's disease: effect on Tau and amyloid pathologies in vitro. *J. Neurochem.* **2015,** *133* (3), 440-451.

33. Abdolazimi, Y.; Lee, S.; Xu, H.; Allegretti, P.; Horton, T. M.; Yeh, B.; Moeller, H. P.; McCutcheon, D.; Armstrong, N. A.; Annes, J. P.; Allegretti, P.; Horton, T. M.; McCutcheon, D.; Smith, M.; Annes, J. P.; Horton, T. M.; Nichols, R. J.; Shalizi, A.; Smith, M., CC-401 promotes β-Cell replication via pleiotropic consequences of DYRK1A/B inhibition. *Endocrinology* **2018**.[online early access] DOI: 10.1210/en.2018-00083. Published Online: March 5, 2018
34. Annes, J. P.; Ryu, J. H.; Lam, K.; Carolan, P. J.; Utz, K.; Hollister-Lock, J.; Arvanites, A. C.; Rubin, L. L.; Weir, G.; Melton, D. A., Adenosine kinase inhibition selectively promotes rodent and porcine islet β-cell replication. *Proc. Natl. Acad. Sci. U. S. A.* **2012,** *109* (10), 3915-3920.
35. Brierley, D. I.; Davidson, C., Developments in harmine pharmacology - Implications for ayahuasca use and drug-dependence treatment. *Prog. Neuro-Psychopharmacol. Biol. Psychiatry* **2012,** *39* (2), 263-272.
36. Airaksinen, M. M.; Lecklin, A.; Saano, V.; Tuomisto, L.; Gynther, J., Tremorigenic effect and inhibition of tryptamine and serotonin receptor binding by β-carbolines. *Pharmacol. Toxicol.* **1987,** *60* (1), 5-8.
37. Fuentes, J. A.; Longo, V. G., Central effects of harmine, harmaline, and related β-carbolines. *Neuropharmacology* **1971,** *10* (1), 15-23.
38. Frost, D.; Meechoovet, B.; Wang, T.; Gately, S.; Giorgetti, M.; Shcherbakova, I.; Dunckley, T., β-carboline compounds, including harmine, inhibit DYRK1A and tau

phosphorylation at multiple Alzheimer's disease-related sites. *PLoS One* **2011,** *6* (5), e19264.

39. Chen, Q.; Chao, R.; Chen, H.; Hou, X.; Yan, H.; Zhou, S.; Peng, W.; Xu, A., Antitumor and neurotoxic effects of novel harmine derivatives and structure-activity relationship analysis. *Int. J. Cancer* **2005,** *114* (5), 675-682.

40. Ishida, J.; Wang, H.-K.; Bastow, K. F.; Hu, C.-Q.; Lee, K.-H., Antitumor agents 201.1 Cytotoxicity of harmine and β-carboline analogs. *Bioorg. Med. Chem. Lett.* **1999,** *9* (23), 3319-3324.

41. Cao, R.; Chen, Q.; Hou, X.; Chen, H.; Guan, H.; Ma, Y.; Peng, W.; Xu, A., Synthesis, acute toxicities, and antitumor effects of novel 9-substituted β-carboline derivatives. *Bioorg. Med. Chem.* **2004,** *12* (17), 4613-4623.

42. Cao, R.; Fan, W.; Guo, L.; Ma, Q.; Zhang, G.; Li, J.; Chen, X.; Ren, Z.; Qiu, L., Synthesis and structure-activity relationships of harmine derivatives as potential antitumor agents. *Eur. J. Med. Chem.* **2013,** *60*, 135-143.

43. Zhang, X.-F.; Sun, R.-q.; Jia, Y.-f.; Chen, Q.; Tu, R.-F.; Li, K.-k.; Zhang, X.-D.; Du, R.-L.; Cao, R.-h., Synthesis and mechanisms of action of novel harmine derivatives as potential antitumor agents. *Sci. Rep.* **2016,** *6*, 33204.

44. Cao, R.; Peng, W.; Chen, H.; Ma, Y.; Liu, X.; Hou, X.; Guan, H.; Xu, A., DNA binding properties of 9-substituted harmine derivatives. *Biochem. Biophys. Res. Commun.* **2005,** *338* (3), 1557-1563.

45. Sobhani, A. M.; Ebrahimi, S.-A.; Mahmoudian, M., An in vitro evaluation of human DNA topoisomerase I inhibition by Peganum harmala L. seeds extract and its β-carboline alkaloids. *J. Pharm. Pharm. Sci.* **2002,** *5* (1), 18-22.

46. Song, Y.; Kesuma, D.; Wang, J.; Deng, Y.; Duan, J.; Wang, J. H.; Qi, R. Z., Specific inhibition of cyclin-dependent kinases and cell proliferation by harmine. *Biochem. Biophys. Res. Commun.* **2004,** *317* (1), 128-132.

47. Cao, M.-R.; Li, Q.; Liu, Z.-L.; Liu, H.-H.; Wang, W.; Liao, X.-L.; Pan, Y.-L.; Jiang, J.-W., Harmine induces apoptosis in HepG2 cells via mitochondrial signaling pathway. *Hepatobiliary Pancreatic Dis. Int.* **2011,** *10* (6), 599-604.

48. Taira, Z.; Kanzawa, S.; Dohara, C.; Ishida, S.; Matsumoto, M.; Sakiya, Y., Intercalation of six β-carboline derivatives into DNA. *Jpn. J. Toxicol. Environ. Health* **1997,** *43* (2), 83-91.

49. Finan, B.; Yang, B.; Ottaway, N.; Stemmer, K.; Mueller, T. D.; Yi, C.-X.; Habegger, K.; Schriever, S. C.; Garcia-Caceres, C.; Kabra, D. G.; Hembree, J.; Holland, J.; Raver, C.; Seeley, R. J.; Hans, W.; Irmler, M.; Beckers, J.; Hrabe de Angelis, M.; Tiano, J. P.; Mauvais-Jarvis, F.; Perez-Tilve, D.; Pfluger, P.; Zhang, L.; Gelfanov, V.; DiMarchi, R. D.; Tschoep, M. H., Targeted estrogen delivery reverses the metabolic syndrome. *Nat. Med.* **2012,** *18* (12), 1847-1856.

50. Luis, S. V.; Burguete, M. I., The Fischer indole synthesis of 8-methyl-5-substituted-1-oxo-β-carbolines: a remarkable high yield of a [1,2]-methyl migration. *Tetrahedron* **1991,** *47* (9), 1737-1744.

51. Roggero, C. M.; Giulietti, J. M.; Mulcahy, S. P., Efficient synthesis of eudistomin U and evaluation of its cytotoxicity. *Bioorg. Med. Chem. Lett.* **2014,** *24* (15), 3549-3551.

52. Thompson, M. J.; Louth, J. C.; Little, S. M.; Jackson, M. P.; Boursereau, Y.; Chen, B.; Coldham, I., Synthesis and evaluation of 1-amino-6-halo-β-carbolines as antimalarial and antiprion agents. *ChemMedChem* **2012,** *7* (4), 578-586.

53. Henderson, J. L.; McDermott, S. M.; Buchwald, S. L., Palladium-catalyzed amination of unprotected halo-7-azaindoles. *Org. Lett.* **2010,** *12* (20), 4438-4441.

54. Lin, G.; Wang, Y.; Zhou, Q.; Tang, W.; Wang, J.; Lu, T., A facile synthesis of 3-substituted 9H-pyrido[3,4-b]indol-1(2H)-one derivatives from 3-substituted β-carbolines. *Molecules* **2010,** *15*, 5680-5691.

55. Fontenas, C.; Bejan, E.; Haddou, H. A.; Galavoine, G. G. A., The Boekelheide Reaction: trifluoroacetic anhydride as a convenient acylating agent. *Synth. Commun.* **1995,** *25* (5), 629-633.

56. Park, K.; Gopalsamy, A.; Aplasca, A.; Ellingboe, J. W.; Xu, W.; Zhang, Y.; Levin, J. I., Synthesis and activity of tryptophan sulfonamide derivatives as novel non-hydroxamate TNF-α converting enzyme (TACE) inhibitors. *Bioorg. Med. Chem.* **2009,** *17* (11), 3857-3865.

57. Song, H.; Liu, Y.; Liu, Y.; Wang, L.; Wang, Q., Synthesis and antiviral and fungicidal activity evaluation of β-carboline, dihydro-β-carboline, tetrahydro-β-carboline alkaloids, and their derivatives. *J. Agric. Food Chem.* **2014,** *62* (5), 1010-1018.

58. Mirza-Aghayan, M.; Boukherroub, R.; Rahimifard, M., A simple and efficient hydrogenation of benzyl alcohols to methylene compounds using triethylsilane and a palladium catalyst. *Tetrahedron Lett.* **2009,** *50* (43), 5930-5932.

59. Soundararajan, M.; Roos, A. K.; Savitsky, P.; Filippakopoulos, P.; Kettenbach, A. N.; Olsen, J. V.; Gerber, S. A.; Eswaran, J.; Knapp, S.; Elkins, J. M., Structures of down syndrome kinases, DYRKs, reveal mechanisms of kinase activation and substrate recognition. *Structure* **2013,** *21* (6), 986-996.

60. Balint, B.; Weber, C.; Cruzalegui, F.; Burbridge, M.; Kotschy, A., Structure-based design and synthesis of harmine derivatives with different selectivity profiles in kinase versus monoamine oxidase Inhibition. *ChemMedChem* **2017,** *12* (12), 932-939.

61. Boursereau, Y.; Coldham, I., Synthesis and biological studies of 1-amino β-carbolines. *Bioorg. Med. Chem. Lett.* **2004,** *14* (23), 5841-5844.

62. Sherman, W.; Day, T.; Jacobson, M. P.; Friesner, R. A.; Farid, R., Novel procedure for modeling ligand/receptor induced fit effects. *J. Med. Chem.* **2006,** *49* (2), 534-553.

63. Friesner, R. A.; Banks, J. L.; Murphy, R. B.; Halgren, T. A.; Klicic, J. J.; Mainz, D. T.; Repasky, M. P.; Knoll, E. H.; Shelley, M.; Perry, J. K.; Shaw, D. E.; Francis, P.; Shenkin, P. S., Glide: A new approach for rapid, accurate docking and scoring. 1. method and assessment of docking accuracy. *J. Med. Chem.* **2004,** *47* (7), 1739-1749.

64. Madhavi Sastry, G.; Adzhigirey, M.; Day, T.; Annabhimoju, R.; Sherman, W., Protein and ligand preparation: parameters, protocols, and influence on virtual screening enrichments. *J. Comput.-Aided Mol. Des.* **2013,** *27* (3), 221-234.

65. Li, J.; Abel, R.; Zhu, K.; Cao, Y.; Zhao, S.; Friesner, R. A., The VSGB 2.0 model: A next generation energy model for high resolution protein structure modeling. *Proteins: Struct., Funct., Bioinf.* **2011,** *79* (10), 2794-2812.

66. LanthaScreen® Eu Kinase Binding Assay - Customer Protocol and Assay Conditions documents located at https://www.thermofisher.com/us/en/home/industrial/pharma-biopharma/drug-discovery-development/target-and-lead-identification-and-validation/kinasebiology/kinase-activity-assays/lanthascreentm-eu-kinase-binding-assay.html. Accessed July 10, 2018

67. Fabian, M. A.; Biggs, W. H.; Treiber, D. K.; Atteridge, C. E.; Azimioara, M. D.; Benedetti, M. G.; Carter, T. A.; Ciceri, P.; Edeen, P. T.; Floyd, M.; Ford, J. M.; Galvin, M.; Gerlach, J. L.; Grotzfeld, R. M.; Herrgard, S.; Insko, D. E.; Insko, M. A.; Lai, A. G.; Lelias, J.-M.; Mehta, S. A.; Milanov, Z. V.; Velasco, A. M.; Wodicka, L. M.; Patel, H. K.; Zarrinkar, P. P.; Lockhart, D. J., A small molecule-kinase interaction map for clinical kinase inhibitors. *Nat. Biotechnol.* **2005,** *23* (3), 329-336.

Table of Contents Graphic

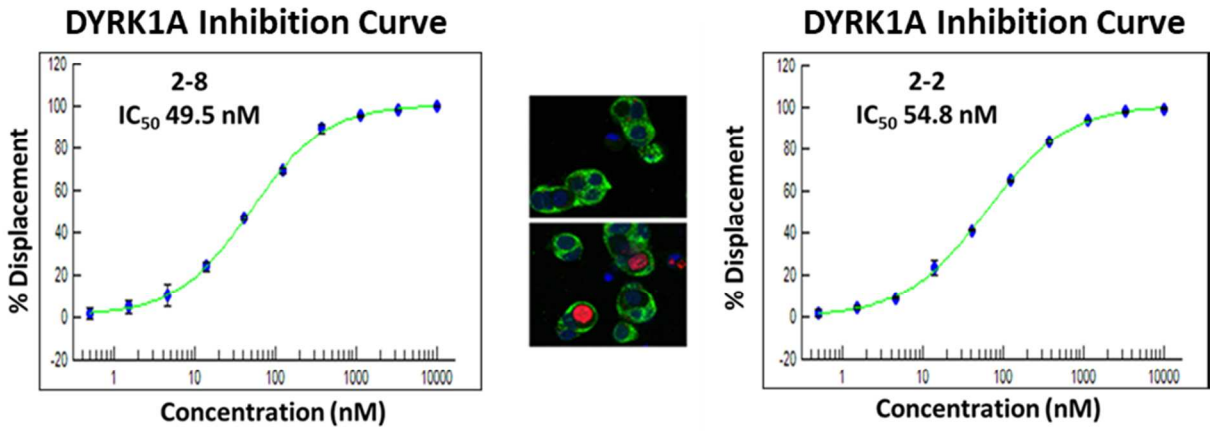

Scheme 1. Synthesis of 1-amino harmine analogs[a]

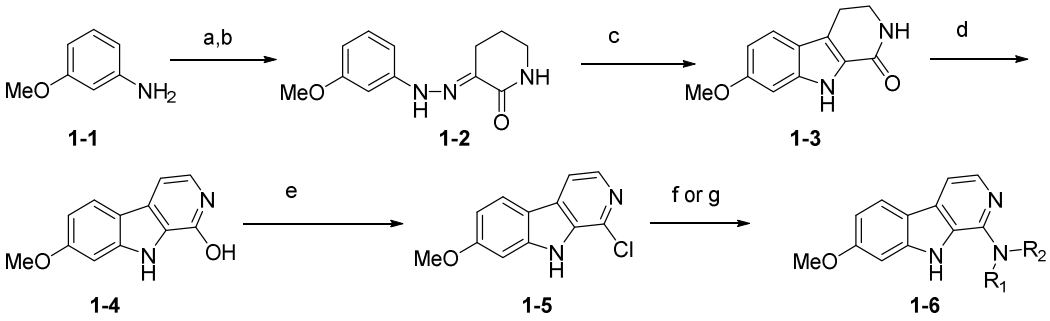

[a]Reagents and conditions: (a) $NaNO_2$ (1.03 eq.), HCl, 10 ^{0}C, 1 h, (b) Ethyl 2-oxopiperidine-3-carboxylate (1.05 eq.), KOH (1.2 eq.), pH adjusted to 4-5, water, rt , 5 h; (c) formic acid, reflux, 1 h; (d) DDQ (1.2 eq.), 1,4-dioxane, 0 ^{o}C-rt, 1 h, 23% (4 step); (e) $POCl_3$, 150 ^{o}C, 24 h, 79%; (f) R_1R_2NH (10 eq.), 170 ^{o}C, 24 h, 43-87% (for **1-6b – 1-6j**); (g) Ruphos (1 mol%), RuPhos Precat (1 mol%), Azetidine (1.2 eq.), LiHMDS (1 M in THF, 2.4 eq.), 90 ^{o}C, 96 h, 31% (based on 32 mg (64%) recovered starting material, for **1-6a**).

Scheme 2. Synthesis of 1-hydroxymethyl and 3-hydroxymethyl harmine analogs[a]

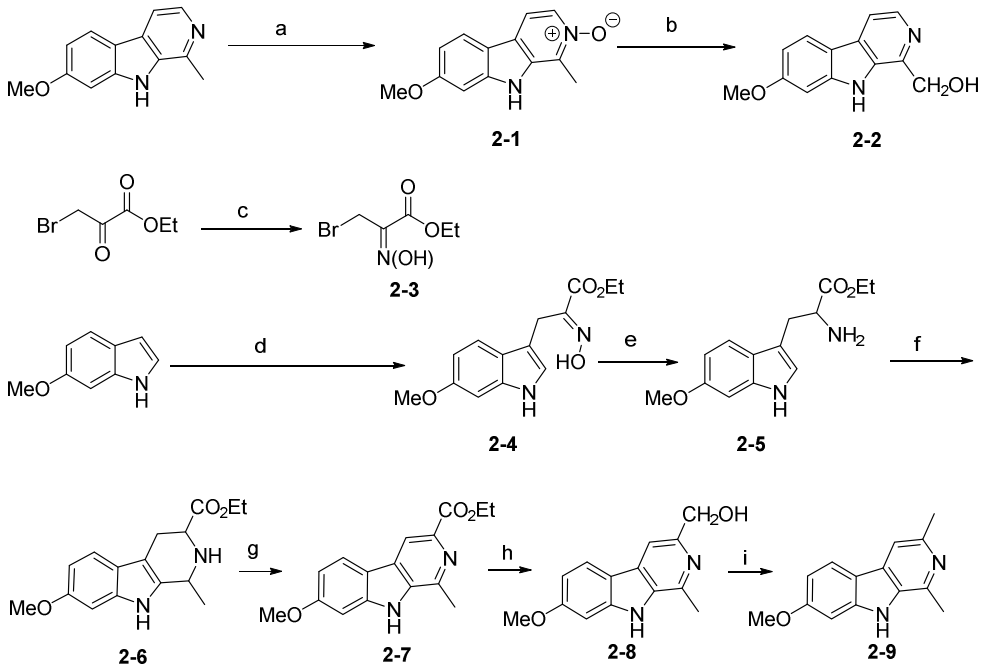

[a]Reagents and conditions: (a) *m*-CPBA (3 eq.), MeOH, $CHCl_3$, 70 °C, 12 h, 47%; (b) TFA anhydride (2.5 eq.), CH_2Cl_2, reflux, o/n, 49%; (c) $N_2H_4OH.HCl$ (1 eq.), MeOH, $CHCl_3$, rt, 24h, 81%; (d) **2-3** (1 eq.), K_2CO_3 (5.5 eq.), DCM, rt, 48 h, 34%; (e) Zn dust, AcOH, rt, o/n, 96%; (f) Acetaldehyde (1 eq.), TFA (5%), DCM, rt, o/n; (g) S_8 (2 eq.), Xylene, reflux,o/n, 75%; (h) $LiAlH_4$ (2 eq.), THF, rt, 12 h, 91%; (i) Et_3SiH (16 eq.), $PdCl_2$ (0.2 eq.), EtOH, 90 °C, 5 h, 27%.

Scheme 3. Synthesis of 1-(1-hydroxy)ethyl and 1-acetyl harmine analogs[a]

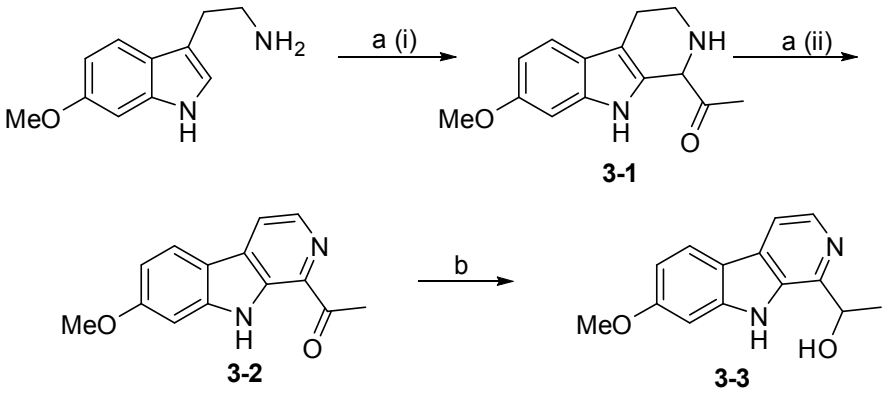

[a]Reagents and conditions: (a) (i) pyruvic aldehyde (1.2 eq.), TFA (5%), DCM, rt, 12 h; (ii) $KMnO_4$ (4 eq.), THF, rt, 12 h, 16% (2 steps); (b) $NaBH_4$ (2 eq.), MeOH, rt, 12 h, 49%.

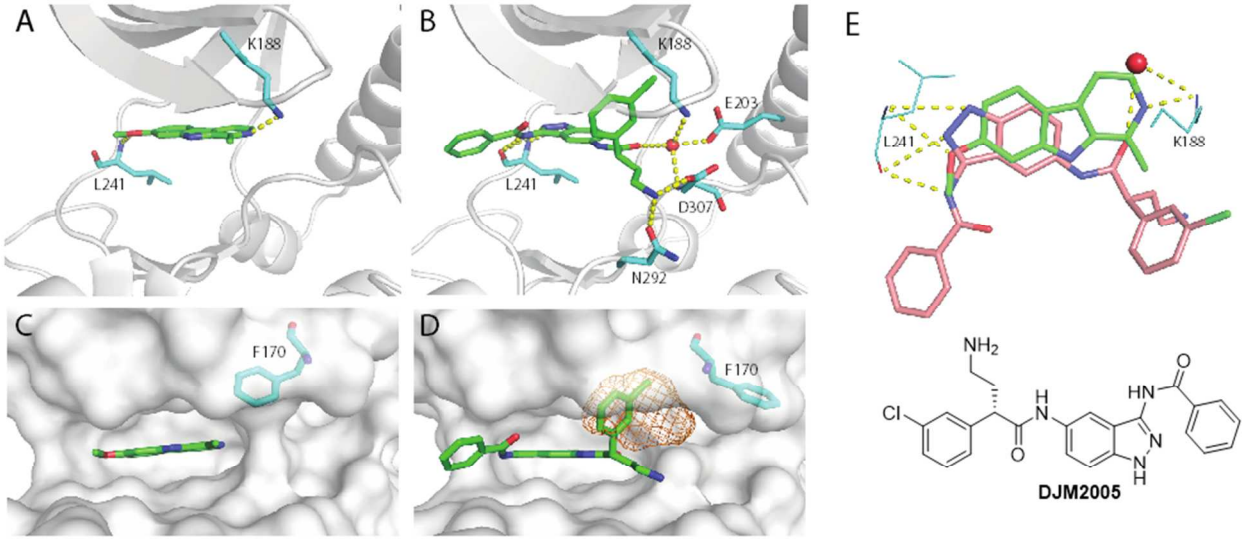

Figure 1. Comparison of Harmine and DJM2005 binding to DYRK1A. **(A)** Harmine binds in the ATP-binding pocket of DYRK1A making hydrogen bonding contacts (yellow dashed lines)

with the side chain of Lys188 and the backbone of Leu241 (PDB 3ANR). **(B)** DJM2005 also interacts with the backbone of Leu241 and makes water-mediated contacts with the side chains Lys188, Glu203 and the backbone of Asp307. Additionally, the primary amino group interacts with the side chain of Asn292 and Asp307 (PDB 2WO6). **(C) (D)** The movement of Phe 170 in the DJM2005 complex (**D**) creates a pocket (orange mesh) that is occupied by the chlorophenyl group of DJM2005. **(E)** Superposition of the harmine (green) and DJM2005 (pink) complexes, highlighting the equivalent hydrogen bonding interactions with Leu241 and Lys188. Orientation is rotated 90 degrees with respect to the view in panels **C** and **D**.

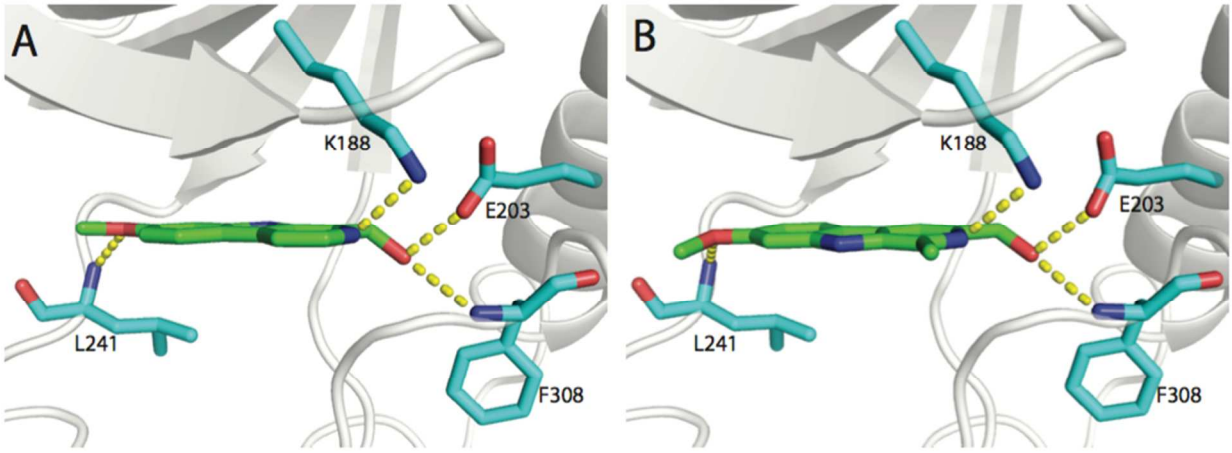

Figure 2. Binding Model of 1-hydroxymethyl harmine Analogs to DYRK1A. (A) Induced fit docking of compound **2-2** predicts that it adopts a binding mode that is distinct from harmine (see **Figure 1A**). The model shows that the hydroxymethyl group at the 1-position causes the scaffold to flip 180^{o} *horizontally*, enabling new putative contacts with the side chains of Glu203 and Phe308, inaccessible to harmine. The model also shows retention of the original hydrogen bonds of harmine 2-nitrogen with Lys188 and 7-methoxy oxygen with Leu241, respectively. Hydrogen bonds are shown as yellow dashed lines. (PDB 3ANR) **(B)** Induced fit docking of compound **2-8** predicts that repositioning of the hydroxymethyl group to position-3 causes this compound to revert to the canonical harmine ATP-site binding mode, while creating new

contacts from the 3-hydroxymethyl group with Glu203 and Phe307 proposed for the "flipped" binding mode for **2-2**. (PDB 3ANR)

Table 1. DYRK1A inhibition and β-Cell proliferation of harmine analogs

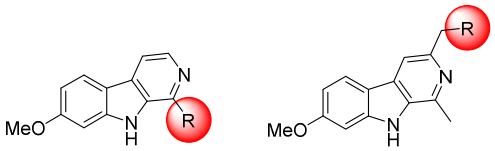

1-4,1-5, 1-6a to 1-6j, 2-2 2-8, 2-9

Compound	R	% DYRK1A inhibition		IC_{50} (nM)[a]	Compound	R	% DYRK1A Inhibition		IC_{50} (nM)[a]
		1000 nM	300 nM				1000 nM	300 nM	
	Harmine	nd	nd	28					
1-6a		89	72	159	1-6i	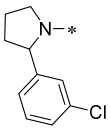	22	1	nd
1-6b		97	90	264					
1-6c		81	57	1500	1-6j	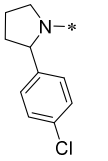	60	27	nd
1-6d		91	71	123					
					1-5		100	98	8.8
1-6e	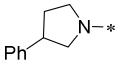	61	34	nd	1-4		38	17	nd
1-6f		84	57	221	2-2	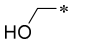	75	49	54.8
					2-8		98	90	49.5
1-6g	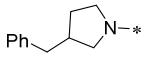	38	15	nd	2-9		-	-	971
1-6h	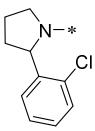	49	12	nd	3-2	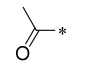	92	85	66.7
					3-3	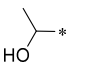	67	38	858

a = IC_{50} values are determined using ten serial three fold dilutions (in duplicate)

nd = not determined

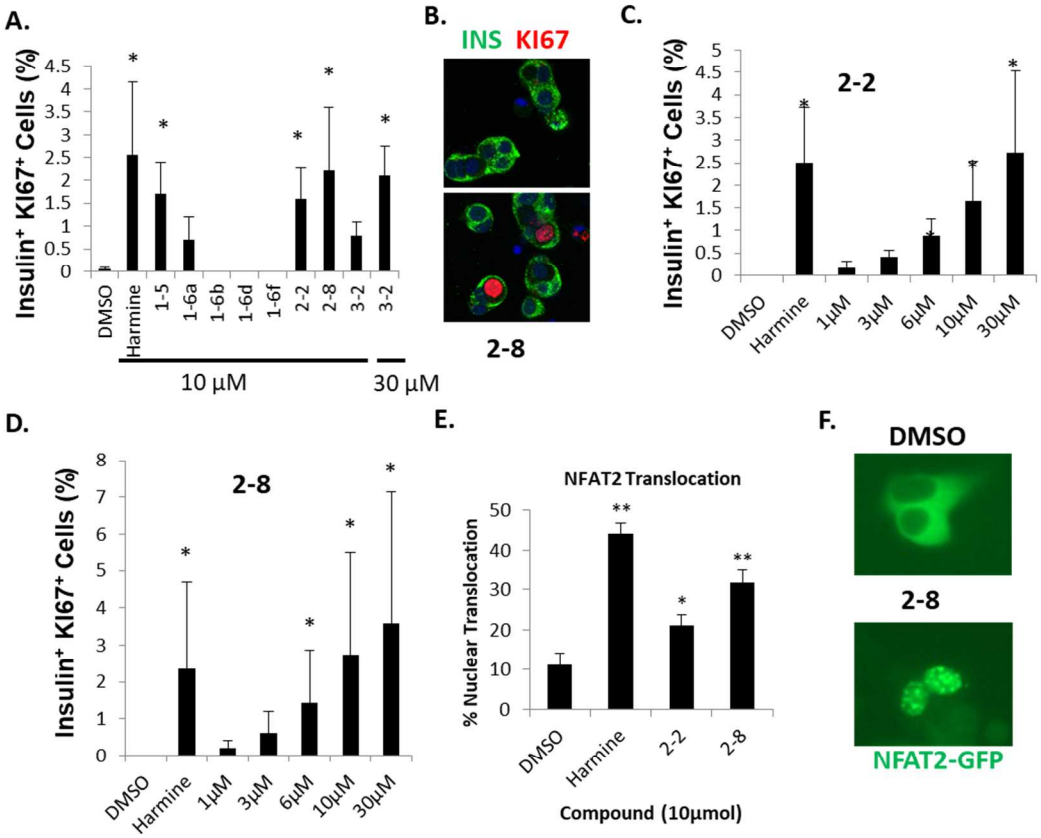

Figure 3. Effects of harmine analogs on human beta cell proliferation. (A) Initial screening of harmine analogs on human beta cell proliferation at 10 µM. DMSO was used as negative control and harmine was used as positive control (n = 4-5). **(B)** A representative example from A of a Ki-67 and insulin double positive cells induced by analog **2-8**. **(C)** and **(D)** Dose-response curves for **2-2** and **2-8** in human β cells (n = 4 for each dose, harmine concentration 10 µM). **(E)** Quantification of nuclear frequency of NFATC1-GFP in R7T1 rodent beta cell lines treated with harmine, **2-2** and **2-8** (10 µM, 24 hr; n = 3 for each compound). **(F)** A representative example of **2-8** (10 µM, 24 hr) increasing the nuclear frequency of NFATC1-GFP in R7T1 rodent beta cells. In all relevant panels, error bars indicate SEM and, * indicates $P < 0.05$. A minimum of 1,000 beta cells was counted for each graph.

Table 2. Kinome scan of compound 2-2, 2-8 and harmine[a]

Target	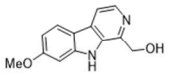 2-2	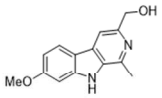 2-8	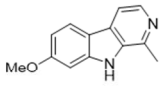 Harmine
CDK11	98	4.8	83
CDK7	27	0.65	21
CDK8	94	0	55
CDKL5	100	6.1	100
CIT	44	8.1	29
CLK1	3.5	7.2	0.35
CLK2	5.5	1.8	2.4
CLK4	17	5	13
CSNK1A1	10	7.8	15
CSNK1D	17	8	13
CSNK1E	6.5	1	1.7
CSNK1G2	30	18	19
CSNK2A1	34	8.3	11
CSNK2A2	37	2.3	23
DAPK1	85	8.8	78
DAPK2	80	2.8	72
DAPK3	81	1.4	69
DRAK2	88	11	73
DYRK1A	0	0	0
DYRK1B	66	0.35	6.1
DYRK2	6.5	4.1	3.2
HASPIN	4.8	0.75	2
HIPK1	30	2.7	21
HIPK2	30	1.3	8.6
HIPK3	21	2.1	9.4
IRAK1	32	18	17
IRAK3	39	70	15
PIK4CB	3.7	19	12
PIM1	65	19	45
PIM2	58	4.7	39
PIP5K2C	28	5	36
RPS6KA4(Kin.Dom.2-C-terminal)	54	1	40
TGFBR2	91	17	78
VPS34	53	28	13

≤ 10
11≤ 20

a = compounds were screened 10 μM against 468 kinases using Discoverx Kinome Scan. Results for primary screen binding interactions are reported as '% DMSO Control', where lower values indicate stronger affinity (see the Supporting Information for details).